Mixed Ionic and Electronic Conduction in Small Molecule Semiconductors

Christina J. Kousseff, Roman Halaksa, Zachary S. Parr and Christian B. Nielsen*

Department of Chemistry, Queen Mary University of London, Mile End Road, London E1 4NS, UK

c.b.nielsen@qmul.ac.uk

Abstract

Small molecule organic semiconductors have displayed remarkable electronic properties with a multitude of pi-conjugated structures developed and fine-tuned over recent years to afford highly efficient hole- and electron-transporting materials. Already making significant impact on organic electronic applications including organic field-effect transistors and solar cells, it is only natural to also consider this class of materials for the emerging field of organic bioelectronics. In efforts aimed at identifying and developing (semi)conducting materials for bioelectronic applications, particular attention has been placed on materials displaying mixed ionic and electronic conduction in order to interface efficiently with the inherently ionic biological world. Such mixed conductors are conveniently evaluated using an organic electrochemical transistor, which further presents itself as an ideal bioelectronic device for transducing biological signals into electrical signals. Here we review recent literature relevant for the design of small molecule mixed ionic and electronic conductors. We assess important classes of p- and n-type small molecule semiconductors, consider structural modifications relevant for mixed conduction and for specific interactions with ionic species, and discuss the outlook of small molecule semiconductors in the context of organic bioelectronics.

Contents

TOC Graphic

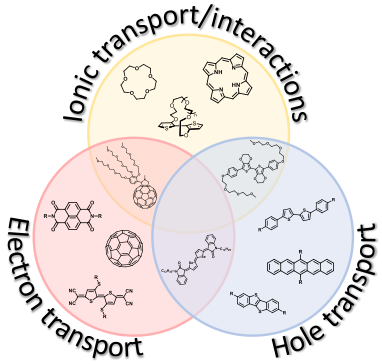

Biographies

Christina Kousseff is a PhD student in the Department of Chemistry at Queen Mary University of London. Before this, she obtained an MRes in Organic Chemistry for Drug Discovery at University College London and a BSc in Biological and Medicinal Chemistry from the University of Exeter. Her current research is focused on the synthesis of semiconducting polymers which are covalently modified for applications in biological sensing.

Roman Halaksa is a PhD student in the Department of Chemistry at Queen Mary University of London. He previously earned his Bachelor's degree from Brno University of Technology in 2015 and a Master's degree from University of Chemistry and Technology, Prague in 2017. His current research is focused on the synthesis and characterization of polymeric organic materials for electronic applications.

Zachary Parr graduated with an MChem from Cardiff University and subsequently completed his PhD at Queen Mary University of London focusing on novel organic semiconductors for biological sensing applications. He has since gone on to undertake postdoctoral posts in the areas of synthetic chemistry relating to novel electronic and photonic materials.

Christian Nielsen received his PhD from the University of Copenhagen in Denmark in 2004. Since 2016, he is leading a research group in the Department of Chemistry at Queen Mary University of London focused on the design and synthesis of new small molecule and polymeric semiconducting materials for organic electronic and bioelectronic applications.

1. Introduction

The broad field of organic electronics is dominated by two classes of materials: molecular and polymeric semiconductors, each with their advantages and disadvantages.[1] While polymers benefit from intra- and interchain transport, relative ease of solution processing when adequately functionalized and a rich synthetic space for chemical modifications, they are often tedious to synthesize and difficult to purify to a high standard and their properties are often sensitive to the polymer's molecular weight and degree of polydispersity. Molecular semiconductors, on the other hand, are typically easier to synthesize and purify and lend themselves to both solution and vacuum deposition techniques. The monodisperse nature of molecular entities allow for straightforward elucidation of structure-property relations although film formation and solid state packing can be very sensitive to small chemical modifications. Together, these two classes of materials have helped to develop a rich research field with important discoveries such as organic light-emitting diodes, solar cells, field-effect transistors and electrochromic devices.[2–8] Those firmly established and commercially mature applications are shaping our society's growing attention towards efficient energy-harvesting and smart electronic devices, while, on the other hand, new emerging applications are also starting to attract significant attention. Amongst these new emerging technologies, the field of organic bioelectronics has gained particular traction over the last decade.[9–11] Using organic electronic materials and devices to interface with biology, organic bioelectronics now encompasses a variety of directions and proof-of-principle applications such as organic electronic ion pumps for local drug delivery, in vivo recordings of brain activity with electrochemical transistors, artificial synapses for neuromorphic computing, and biofuel powered glucose detection in bodily fluids.[12–15] Many bioelectronic applications have relied on the organic electrochemical transistor (OECT), first developed by White *et al.* in 1984, taking advantage of a typical three-electrode transistor geometry that can be directly interfaced with a biological system via the aqueous electrolyte solution used for electrochemical gating.[16–19]

The benefits of soft organic materials with a high degree of biocompatibility combined with relatively simple, cheap and scalable device fabrication methods have helped advance the field at a

fast pace and in numerous directions over the last decade. Limited nevertheless by a narrow selection of active materials originally developed for other applications, including polyaniline, polypyrrole and poly(3,4-ethylenedioxythiophene):polystyrene sulfonate (**PEDOT:PSS**),[16,20–22] contributions from synthetic chemists in the form of new tailor-made materials have been steadfastly pursued over the last five years.[23–26] Aided by the many bioelectronic applications available and the close resemblance to the wider studied organic field-effect transistor (OFET) in terms of active materials design, focus has predominantly been on the design and synthesis of new active materials for the OECT. This has led to the pursuit of organic semiconductors that are able to conduct both electronic and ionic charges in the bulk. Using thoroughly established design motifs from the organic electronics community, such as the electron-rich polythiophene scaffold and electron-deficient naphthalene diimide polymers for p- and n-type electronic charge transport respectively, the additional need for ionic conduction has mainly been addressed through side chain modifications.[27,28] As a consequence, the field now has a steadily growing family of tailor-made p- and n-type polymers, often classified as organic mixed ionic-electronic conductors (OMIECs), fulfilling the fundamental requirements for effective OECT operation with several reviews providing excellent overviews of recent materials developments.[29,30] Molecular semiconductors, on the other hand, have been somewhat overlooked in the context of organic bioelectronics and mixed conduction despite the often excellent electronic charge transport reported for instance in OFETs. Here, we will discuss briefly the premise for electronic charge transport in molecular semiconductors and highlight examples of efficient charge transport in molecular systems from recent literature. With a subsequent focus on ionic conduction, we will critically analyze various approaches to endow molecular semiconductors the ability to interact with ionic species. Looking subsequently at the dual requirement of mixed ionic and electronic conduction, we will discuss recent successful efforts developing molecular OMIECs and incorporating them into OECTs as well as future directions for molecular semiconductors in bioelectronic applications.

2. Electronic conduction in small molecule semiconductors

Detailed descriptions of charge transport in molecular semiconductors and exhaustive overviews of p- and n-type semiconductor structures are present in abundance in the scientific

literature,[31–33] so here we will merely highlight the most important aspects to consider in order to design and understand molecular semiconductors for charge transport applications.

2.1 Charge transport

Moving from an isolated conjugated molecular system to an assembly of molecules in the solid state, we must consider the interactions between the delocalized π-electron systems of each molecule that are ultimately responsible for the conduction of charges. As illustrated in Figure 1a-b for sexithiophene (**6T**), the electronic coupling described by the transfer integral *J*, decays exponentially with the intermolecular π-stacking distance of two cofacial π-conjugated molecules.[34] Long axis displacement, on the other hand, results in an oscillation behavior and together these two examples already point towards a strong interplay between charge transport and molecular assembly in the solid state. Large transfer integrals, coupled with a low degree of energetic disorder and small electron-phonon coupling, lead to more delocalized charges and therefore more effective intermolecular charge hopping.[35] While the charge hopping model is often used to describe charge transport in molecular semiconductors, band-like transport has also been experimentally observed for several molecular semiconductors.[36,37] Increasing charge carrier mobility with decreasing temperature is characteristic of band-like transport whereas charge hopping is a thermally activated charge transport process.[38,39]

Crystalline molecular semiconductors are found to assemble in different configurations such as the slipped stack, brick wall, slipped π-stack and herringbone packing motif, with the latter two illustrated in Figure 1c for well-known semiconductors rubrene and benzothieno[3,2-*b*][1]benzothiophene (**BTBT**).[40] While the slipped stack motifs often have only one dominant transfer integral and strongly anisotropic transport properties, herringbone packing is often characterized by three significant transfer integrals, thus affording a higher degree of isotropic charge transport in the x-y plane, with brick wall packing falling in between those two extremes with two significant transfer integrals. Although single-crystal OFETs have been fabricated, thin continuous films deposited by various scalable coating techniques are preferred for most practical applications of molecular

semiconductors. Therefore, it is crucial also to consider carefully the orientation and alignment of crystalline domains and the grain boundaries between crystalline domains within the semiconductor thin film. Distinguishing broadly between soft (low-angle) and hard (high-angle) grain boundaries, exemplified for a slipped stack configuration in Figure 1e, high-angle grain boundaries are particularly detrimental to charge transport across neighboring domains.[41] Slipped stack materials with only one dominant transfer integral are furthermore expected to be more sensitive to crystallographic misorientation than, for example, a herringbone motif with three significant transfer integrals.

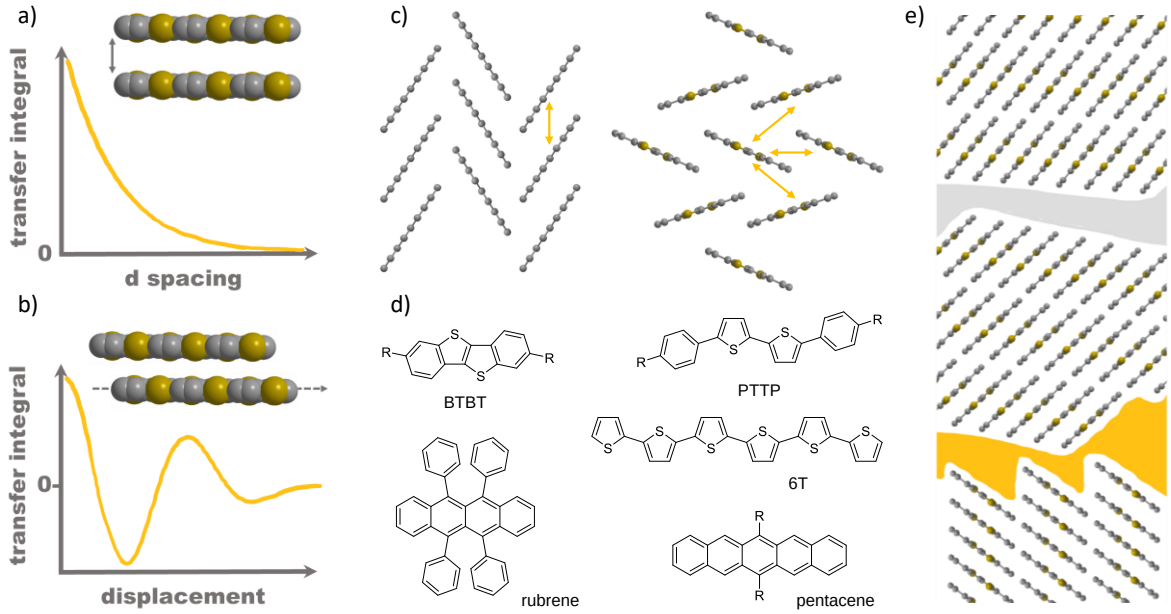

Figure 1 Qualitative relationship between transfer integral and (a) d-spacing and (b) long-axis displacement for sexithiophene. Adapted with permission from ref. [34]. Copyright (2002) National Academy of Sciences, U.S.A.; slipped π-stack and herringbone packing motifs with dominant transfer integrals (c); popular p-type molecular semiconductors (d); illustration of soft and hard grain boundaries (e, adapted with permission from ref. [41], Copyright 2009 Nature Publishing Group).

In regard to electronic conduction, we furthermore distinguish between p-type charge transport, where electron holes are the dominant charge carriers, and n-type charge transport, where electrons represent the dominant charge carriers. Hole (p-type) transport requires charge injection, for instance from an energetically aligned metal electrode, into the highest occupied molecular orbital (HOMO) whereas n-type semiconductors conduct following charge injection into the lowest unoccupied molecular orbital (LUMO). Charge injection, whether p-type or n-type, results in the

formation of polarons which are mobile charged species delocalized across several π-conjugated bonds in the semiconductor. Polarons represent a polarization as well as a distortion of the lattice, often seen as a rearrangement of double bonds towards a quinoidal structure (or quinoidal-like structure for non-benzoid systems). High charge carrier concentration can furthermore lead to the formation of bound polaron pairs, known as bipolarons, which are often less mobile than the corresponding polarons.[42] As indicated, generation of free charge carriers requires energetic alignment, whether it is caused for instance by a metal electrode, a chemical dopant or an electrochemical potential. This necessitates control of frontier energy levels which can be accomplished through molecular design, as will be discussed more extensively below. The molecular semiconductors displayed in Figure 1d are all p-type materials (i.e. found to work as the active material in a p-type transistor) with relatively low ionization potentials and thus energetically accessible HOMO levels. More electron-deficient molecular semiconductors with high electron affinities and therefore suitable LUMO levels are also abundant, with many displaying excellent n-type charge transport behavior. One of the figures of merit used to evaluate charge transport behavior is the charge carrier mobility, μ, commonly extracted from OFET device characteristics although other approaches such as time-of-flight techniques and the space-charge limited current technique are also applied. Extracted values of hole (μ_h) and electron (μ_e) mobilities are strongly dependent on the measurement technique as well as exact device fabrication methods, while it is also worth mentioning that non-ideal semiconductor behavior can lead to overestimated charge carrier mobilities.[43,44,33,45]

2.2. Hole-transporting molecular semiconductors

Fused aromatic systems such as rubrene and various pentacene derivatives (Figure 1d) are among the most studied p-type molecular systems. Rubrene, in the form of single crystals grown from the vapor phase, displays very high OFET mobilities in the range 20-40 cm^2/Vs despite adapting a slipped π-stack arrangement with only one dominant transfer integral.[38,46,47] While unsubstituted pentacene (Figure 1d, R = H) adopts a herringbone packing motif, TIPS-pentacene (R = C≡C-Si(iPr)$_3$) with bulky solubilizing groups distanced from the center of the pentacene core by rigid alkyne spacers, packs in a brick wall arrangement.[48] TIPS-pentacene represents an early example of a

successful transformation of an insoluble molecular semiconductor into a solution processable derivative through molecular design while maintaining structural organization conducive to charge transport (μ_h ~ 1 cm^2/Vs). Further chemical design has led to a number of related materials, with the difluorinated anthradithiophene derivative **diF-TES-ADT** (Figure 3) a notable example with a hole mobility of 6 cm^2/Vs, which has been further improved to above 19 cm^2/Vs in OFETs with reduced contact resistance.[49–51]

Thiophene-based materials also play a large role in p-type molecular semiconductors, from early simple structures like **PTTP** to more synthetically challenging fused compounds like **BTBT** and its extended derivatives. Amongst a series of phenylene-thienylene based discrete oligomers of different length, **dH-PTTP** (Figure 1d, R = *n*-hexyl) displayed the highest hole mobility, approaching 0.1 cm^2/Vs measured on vacuum-deposited films, with only slightly inferior performance observed with solution-processed thin films.[52] **BTBT** can be viewed as a fully fused derivative of **PTTP**. It has appeared as a versatile molecular semiconductor showing high tolerance with respect to the peripheral substituents (R = phenyl, *n*-octyl, *n*-dodecyl) that endow solution processability, with multiple derivatives affording OFET mobilities in the range 1 – 2 cm^2/Vs.[53,54] Merging large-area solution processing with the advantages of single-crystal transistors, Minemawari *et al.* integrated the anti-solvent crystallization technique into an inkjet printing protocol using **C$_8$-BTBT** (R = *n*-octyl) as the active semiconductor.[55] Printing first the anti-solvent, dimethylformamide, immediately overprinted with **C$_8$-BTBT** in 1,2-dichlorobenzene, slow solvent evaporation subsequently facilitates growth of highly uniform and crystalline **C$_8$-BTBT** thin films at the air-liquid interface. When tested in field-effect devices, this afforded saturated hole mobilities as high as 31 cm^2/Vs with an average value of 16 cm^2/Vs. In a comparative study of vapor-deposited films of **C$_8$-BTBT**, **C$_{10}$-BTBT**, and **C$_{12}$-BTBT**, charge transport properties were found to improve with increasing chain length irrespective of OFET substrate treatments.[56] Careful evaluation of the isostructural packing motifs gave evidence of stronger hydrophobic interactions with increasing chain length which in turn result in increased intermolecular interactions of the aromatic cores, thus explaining the superior p-type characteristics for devices with **C$_{12}$-BTBT** as the active channel material. In agreement with this work, a theoretical

study found the dominant transfer integrals to increase significantly when going from **C_8-BTBT** to **C_{12}-BTBT** resulting in a predicted more than two-fold increase in charge carrier mobility.[57] In the same study, the heavier chalcogen-derivative **BSBS**, with selenium replacing sulfur, was also investigated and predicted to outperform the sulfur-analogue significantly. Experimentally, however, **BSBS** has been less studied than **BTBT**, not least owing to its much more challenging synthesis, and so far its charge transport properties are still lagging behind.[53,58] With the limited synthetic freedom to modify the **BTBT** core straightforwardly, much research has instead focused on elongated fused derivatives such as **DNTT** where the two benzene rings are substituted for naphthalenes. Exploring **C_n-DNTT** with n = 6, 8, 10, and 12, Kang *et al.* found **C_{10}-DNTT** to possess the best charge transport properties in evaporated OFETs, with hole mobilities approaching 8 cm^2/Vs after careful device optimization.[59] Comparing fused aromatic systems such as **BTBT** and **DNTT**, that have alkyl chains parallel to the long axis of the molecule, with e.g. rubrene and TIPS-pentacene, where the substituents are parallel to the short axis of the molecule, Sirringhaus and co-workers found a lower degree of dynamic disorder stemming from intermolecular thermal vibrations with lower amplitudes for the long-axis molecular design.[35] Nevertheless, such linear or quasi-linear structures with long-axis substitution are still capable of and sensitive to translational and rotational molecular vibrations. Displacement in the long-axis direction, in particular, has been found to have a significant impact on the degree of disorder, in some cases contributing more than 80% to the total thermal disorder.[60] The importance of this level of understanding and its correlation to structure-property relations has been further highlighted by comparing unsubstituted **DNTT** and **C_8-DNTT**; despite significantly larger transfer integrals for the alkylated compound in line with discussions above, enhanced thermal disorder by long-axis displacement cancels much of the expected gain when comparing with unsubstituted **DNTT**. From a molecular design point of view, arguments can be made that changing from these linear π-conjugated cores to more bent-shaped structures can lead to suppressed molecular vibrations and thus offer a route to decrease energetic disorder and obtain higher performing charge transport materials.[61] Fully fused and highly crystalline semiconductors such as **BTBT** and **DNTT** are sensitive to processing conditions including for instance choice of substrate and deposition conditions, which can lead to different polymorphs with vastly different charge transport properties as seen for

example for a fused BTBT-derivative where the α-phase crystal gives rise to a maximum OFET hole mobility of 8.5 cm^2/Vs while the β-phase crystal performs significantly better with a maximum hole mobility of 18.9 cm^2/Vs.[62] Annealing conditions are likewise critical, with both solvent vapor annealing and thermal annealing found to influence microstructure, crystal quality and hence charge transport properties.[36,63]

2.3 Electron-transporting molecular semiconductors

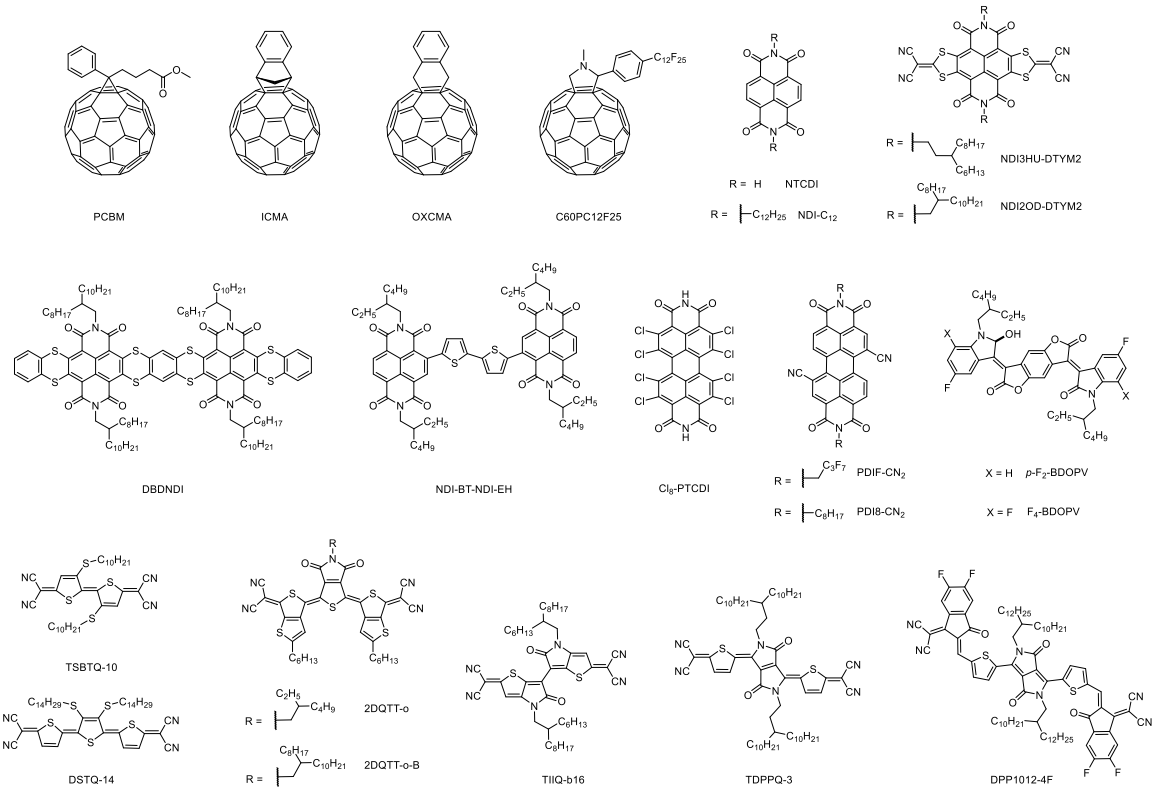

Figure 2 Examples of electron-transporting molecular semiconductors.

Efficient electron transporting (n-type) systems are highly desirable for many device applications, but are less prevalent in the literature than p-type materials due the characteristic instability of organic anions in ambient conditions as a result of charge carrier trapping.[64,65] Materials with an electron affinity (EA) above 4.0 eV are generally not prone to oxidation by H_2O and O_2; hence, a LUMO level of below -4.0 eV is often considered a benchmark which may afford n-type materials operational stability in air.[66] Over the last several years, the rational design of small molecules exhibiting sufficiently low LUMO levels for this purpose has produced a variety of promising materials. In

particular, several cores feature prominently in the field, upon which much work has been done to optimize electron mobility and LUMO level. Discussed herein are fullerene derivatives, rylene diimides, benzodifurandione-based oligo(p-phenylene vinylene) (**BDOPV**) and quinoidal oligothiophenes.

Some of the first and most well-known electron deficient building blocks to have been used as electron-transporting materials are fullerenes and their derivatives, dominating the field of bulk heterojunction solar cells for many years,[67] in particular, the solution-processable [6,6]-phenyl C_{61}- butyric acid methyl ester (**PCBM**, Figure 2).[68] Despite their ubiquity, many materials of this type do not exhibit sustained air stability or high electron mobility, even including **PCBM**, which, despite a low LUMO level reported in the region of -3.7 eV to -4.3 eV,[69,70] tends towards an amorphous structure, thereby enabling the diffusion of H_2O and O_2 into the channel layer allowing charge trapping to occur,[71] while also reducing electron mobility.[72]

A variety of adaptations have been successfully applied to circumvent these issues. For non-covalently-modified C_{60}, crystallinity has been variously improved by incorporation of a pentacene monolayer for advanced wetting control (μ_e = 4.9 cm^2/Vs);[73] deposition by hot wall epitaxy (μ_e = 6 cm^2/Vs);[74] and large-area single crystal growth by droplet-pinned crystallization (μ_e = 11 cm^2/Vs).[75] For covalently-modified C_{60} derivatives, mobility and air stability have been studied extensively. A number of factors affecting electron delocalization and film microstructure, such as fullerene size, covalent modification, and deposition method, are of consideration in achieving fullerene-based films of high performance; a fine balance of all of these properties is therefore required to achieve optimal mobility and stability. In 2012, work by Li *et al.* investigated the effect of fullerene size, and adduct number and type, on mobility. The authors note the multiple factors at play which affect electron mobility: C_{60}, rather than C_{70}, fullerene size was preferable due to the more complete electron delocalization of the former; while mono-, rather than bis- or tris- covalent functionalization is advantageous due to its comparatively minor perturbation of the film microstructure. In addition, they note that while surface defects were observed in some films as spun from chloroform, in this case electron mobility was not restricted due to comparative film thickness, and thermal annealing was therefore not required.[76] Although the

aforementioned study finds decreasing fullerene size to from C_{70} to C_{60} to be preferable in terms of mobility, conflicting properties in these complex systems mean that the identification of straightforward trends for optimal operation is not always possible: Anthopoulos and colleagues note that increasing fullerene size from C_{60} to C_{84} invites operation in ambient conditions due to the relative stability of the **[84]PCBM** anion (LUMO = -4.0 eV, $\mu_e = 0.5 \cdot 10^{-3}$ cm^2/Vs over several months in air); and in this case, mobility increases more than sixfold (to $\mu_e > 3 \cdot 10^{-3}$ cm^2/Vs) for thermally annealed films due to reduced contact resistance at the Au/**[84]PCBM** interface, while recrystallization was shown to have a negligible effect on film structure, but to produce the best operating characteristics nonetheless.[77] Meanwhile, Yu *et al.* induce air stability into C_{60} fullerene systems by covalent modification with the incorporation of indene (**ICMA**, Figure 2, LUMO = -3.88 eV) or *o*-xylenyl (**OXCMA**, Figure 2, LUMO = -3.85 eV) mono-adducts, to give mobilities of μ_e = 0.05 and 0.04 cm^2/Vs respectively in air for solution-sheared films. They attribute this to the prevention of O_2 and H_2O diffusion as a result of improved molecular packing.[78] Similarly, Chikamatsu *et al.* demonstrate that perfluoroalkyl side chains are able to act as a protective gas barrier; crystalline films of **C60PC12F25** (Figure 2) show superior mobility and air stability compared to amorphous **PCBM** deposited in the same conditions, despite a higher LUMO value (**C60PC12F25** LUMO = -3.63 eV, μ_e = 0.25 cm^2/Vs under vacuum, 0.08 cm^2/Vs in air; **PCBM** LUMO = -3.66 eV, μ_e =0.025 0.25 cm^2/Vs under vacuum, inactive in air).[71] Despite these advances, in recent years, much interest has been directed towards the development of alternative small molecule n-type materials, both as active transistor materials and for organic solar cells in the form of non-fullerene acceptors.[79,80] While fullerene chemistry is often very challenging and limited in scope, non-fullerene n-type materials, such as those discussed below, lend themselves more easily to synthetic adaptation and large-scale manufacture, and have the potential for innately superior ambient stability, possessing lower LUMOs by molecular design.

One of the most popular motifs among non-fullerene electron-transporting semiconductors is that of the rylene diimides. The structure, featuring electron withdrawing imide moieties proximal to a π-conjugated aromatic core, provides these diimides with the characteristic low LUMO and high mobility levels required for application as an n-type channel layer in transistor devices. Specifically, naphthalene

diimides (**NDI**s) and the analogous perylene diimides (**PDI**s) featuring an extended π-conjugated core, are the most extensively researched for use in this area.[81] The first reported application of an NDI species in an OFET gave a mobility in the order 10^{-4} cm^2/Vs, for **NTCDI** (Figure 2, R=H) under vacuum.[82] Recently, a range of innovative structural modifications have resulted in the creation of **NDI**-based materials with the potential for improved performance in transistor devices, by ways such as decreased LUMO, or improved mobility, solution processability or stability under ambient conditions.

The introduction and modification of side chains in rylene diimides can affect their transistor performance, in addition to enabling solution processability. In 2019, Welford *et al.* conducted a systematic investigation into the effect of side chain length and type on electron mobility in a series of **NDI** small molecules.[83] Linear side chains in increasing length from C_4 to C_{12}, plus a branched 2-ethylhexyl chain, were installed at both *N* positions, and OFET electron mobility was measured. Previous calculations by Ma *et al.* had predicted a decrease in mobility corresponding to increasing linear alkyl chain length in NDIs, a result of charge transfer integral reduction related to changes in displacement along the short axis in the π-π stacking configuration of the series.[57] While this effect was observed experimentally for chain lengths below C_6, Welford *et al.* found that conflicting factors, such as improving thin film morphology, caused the trend to reverse for increasing lengths above this size. In fact, the maximum value experimentally obtained was for the longest chain included in the study, **NDI-C_{12}** (Figure 2), with a mobility of μ_e = 0.19 cm^2/Vs for a blade-coated OFET. Additionally, inclusion of the branched chain was found to produce a mobility among the lowest in the series (μ_e = 0.068 cm^2/Vs), attributed to disruption of film uniformity.[83] Therefore, while molecular packing is important, the achievement of optimal mobility via side chain engineering is a complex matter due to the consideration of sometimes conflicting factors such as crystallinity, grain size and film morphology. Fluorination of side chains is another approach which can alter molecular packing and transistor performance; *para*-fluorination of *N,N'*-diphenyl **NDI** has been shown to invoke a change from stacking in a π-π motif to herringbone, with theoretical electron transfer calculations showing slightly higher mobility for the fluorinated version.[84] For PDIs, Stoeckel *et al.* found that fluorination of alkyl side chains in **PDI-CN_2** had a marked effect on charge transport mechanisms, and therefore mobility,

switching from band-like charge transport for **PDI8-CN$_2$** to thermally activated for **PDIF-CN$_2$** (Figure 2).[85]

In addition to alkyl chain adaptations, modification to the core of rylene diimides can substantially affect their properties. Incremental thionation of **PDI** has been shown to improve electron affinity;[86] while full chlorination of the aromatic core (**Cl$_8$-PTCDI**, Figure 2) enables the achievement of LUMO values exceeding the required value for air stability (-4.23 eV) thereby affording mobility in air up to μ_e = 0.82 cm^2/Vs.[87]

In 2018, Ha *et al.* employed Stille coupling to create a bis-**NDI** featuring a rotatable central bithiophene linker, which improved solution processability while maintaining good OFET properties (**NDI-BT-NDI-EH**, Figure 2, μ_e = 0.016 cm^2/Vs, LUMO = -4.04 eV).[88] The following year, Luo *et al.* synthesized core-expanded bis-**NDI**s of which the best performing, **DBDNDI** (Figure 2), exhibited mobility up to μ_e = 0.02 cm^2/Vs in air and a LUMO of -4.05 eV.[89] Another core-expanded **NDI**, (1,3-dithiol-2-ylidene)malononitrile (**NDI2OD-DTYM2**, Figure 2) displayed highly air- and temperature-stable device performance, with mobility achieved up to μ_e = 1.2 cm^2/Vs in ambient conditions.[90] Combining side chain and core modification, Zhang *et al.* then used this already high-performing core structure to investigate the effect of alkyl chain branch position and length on OFET properties. The highest recorded mobility of μ_e = 3.5 cm^2/Vs was achieved for **NDI3HU-DTYM2** (Figure 2), which featured C_{11} alkyl chains with a C_6 branch at the 3-position, and this was attributed to an optimized balance between π-π proximity, hydrophobic chain interactions, and steric hindrance to give ideal molecular packing, while maintaining high crystallinity and solution processability.[91]

Benzodifurandione-based oligo(p-phenylene vinylene) (**BDOPV**) was first developed in 2013 as a monomer which, when incorporated into a polymer, improved upon the high LUMO and low mobility of previously studied poly(*p*-phenylene vinylene)s (**PPV**s), due to its electron withdrawing and H-bonding carbonyl groups.[92] Shown to be an effective n-type small molecule for OFET application when fluorinated,[93] a systematic examination of the effect of fluorination on the crystal packing and mobility of ethylhexyl **BDOPV**s was carried out in 2015 by Dou *et al.*. The two best-performing materials, **F$_4$-**

BDOPV and ***p*-F$_2$-BDOPV** (Figure 2), demonstrated maximum electron mobilities of μ_e = 12.6 and 6.55 cm^2/Vs respectively, which was attributed to improved electron transfer as a result of an antiparallel, cofacial stacking arrangement. This was in contrast to herringbone packing adopted for ***o*-F$_2$-BDOPV**, and slipped 1D stacking for **BDOPV** and **F$_6$-BDOPV**. While all of the materials displayed similar interplanar π-π distances in the range 3.25-3.43 Å, the antiparallel cofacial arrangement enabled the shortest displacements along the molecular axes, and therefore, the highest transfer integrals. Quoted mobility values were measured in ambient conditions, and all fluorinated **BDOPV** materials demonstrated good stability in air.[94] This is attributed to the combined effects of the electron-withdrawing fluorine facilitating LUMO values of -3.84 eV or lower, and the dense molecular packing providing a kinetic barrier against the diffusion of atmospheric oxidant species.[93]

Another widely-used approach to the design of n-type small molecular semiconductors is the development of stable quinoidal systems. Specifically, quinoidal dicyanomethylene-terminated oligothiophenes display suitable electron-accepting characteristics due to the high electron affinity of the quinoidal backbone, while the dicyanomethylene groups contribute to planarity for good mobility, and to desirable LUMO levels by their electron withdrawing effect.[95] These properties were first explored by Pappenfus *et al.* in 2002, who applied a butyl terthiophene quinoid in an OFET for the first time, obtaining a mobility of $5 \cdot 10^{-3}$cm^2/Vs.[96] This framework has been developed to considerable effect, with many structural modifications affording improved OFET characteristics. Recent highlights include the incorporation of thioalkyl chains along the backbone, which enhances planarity via intramolecular S-S interaction. In 2020, Joseph *et al.* achieved LUMO -4.36 eV and μ_e = 0.18 cm^2/Vs (**TSBTQ-10**, Figure 2) by applying this modification to quinoidal dicyanomethylene bithiophenes, which displayed herringbone packing ideal for π-orbital interaction.[97] The same year, Vegiraju *et al.* installed thioalkyl chains to the central unit of a terthiophene analogue, which encouraged a pseudo-fused pentathienoacene structure and thereby permitted the adoption of a favorable slipped π-π stacking arrangement (LUMO -4.28 eV, μ_e = 0.77 cm^2/Vs in air for **DSTQ-14**, Figure 2).[98]

Expanding π-conjugation via the inclusion of fused-ring systems has been shown to improve OFET characteristics in quinoidal systems; in 2014, Zhang *et al.* adapted dicyanomethylene terthiophene by

replacing the central thiophene unit with thienopyrrolodione and the outer two with thienothiophene, creating an A-D-A-D-A system which demonstrated LUMO -4.51 eV, and μ_e up to 3.0 cm^2/Vs in air (**2DQTT-o**, Figure 2).[99] The same group later went on to examine the effect of alkyl chain branching and sulfur orientation within the molecular framework of these materials, finding that branched chains were preferable over linear for the formation of highly crystalline films, while distal sulfur orientation encouraged 3D packing, to give μ_e as high as 5.2 cm^2/Vs in air (LUMO -4.44 eV) for **2DQTT-o-B** (Figure 2).[100] Furthermore, Davies *et al.* have shown that crystal polymorphism can strongly impact electron mobility; using solution printed films of **2DQTT-o-B**, the authors identified five distinct polymorphs with different unit cell structures and crystal packing which yielded substantially different electron mobilities. The best of these, a film annealed at 100 °C, demonstrated a mobility of 0.22 cm^2/Vs, superior by five orders of magnitude to the same material when annealed at 210 °C, thus demonstrating the importance of fabrication method and polymorph control for small molecular n-type transistors.[101] This year, another fused-ring quinoidal system based on thienoisoindigo was developed by Velusamy *et al*., with the branched-alkyl substituted **TIIQ-b16** (Figure 2) recording mobility up to μ_e = 2.54 cm^2/Vs and a LUMO of -4.16 eV as a result of close face-to-face π-π stacking.[102] The inclusion of the highly planar, electron deficient diketopyrrolopyrrole (**DPP**) moiety is an alternative successful approach; in 2015, Wang *et al.* synthesized a family of quinoidal small molecules featuring dicyanomethylene-thiophenes flanking a central alkylated **DPP**, to create highly crystalline films with close in-plane π-π stacking, the best performing of which, **TDPPQ-3** (Figure 2), demonstrated LUMO -4.50 eV and μ_e = 0.72 cm^2/Vs in air.[103] In 2019, Zhou *et al.* further extended this system by end-capping an analogue with fluorinated 3-(dicyanomethylidene)-indan-1-one. The resulting material, **DPP1012-4F** (Figure 2), displayed a LUMO of -4.21 eV and μ_e up to 1.05 cm^2/Vs under nitrogen or 0.88 cm^2/Vs in air, despite its non-quinoidal form.[104]

2.4. Charge transport in molecule:polymer blends

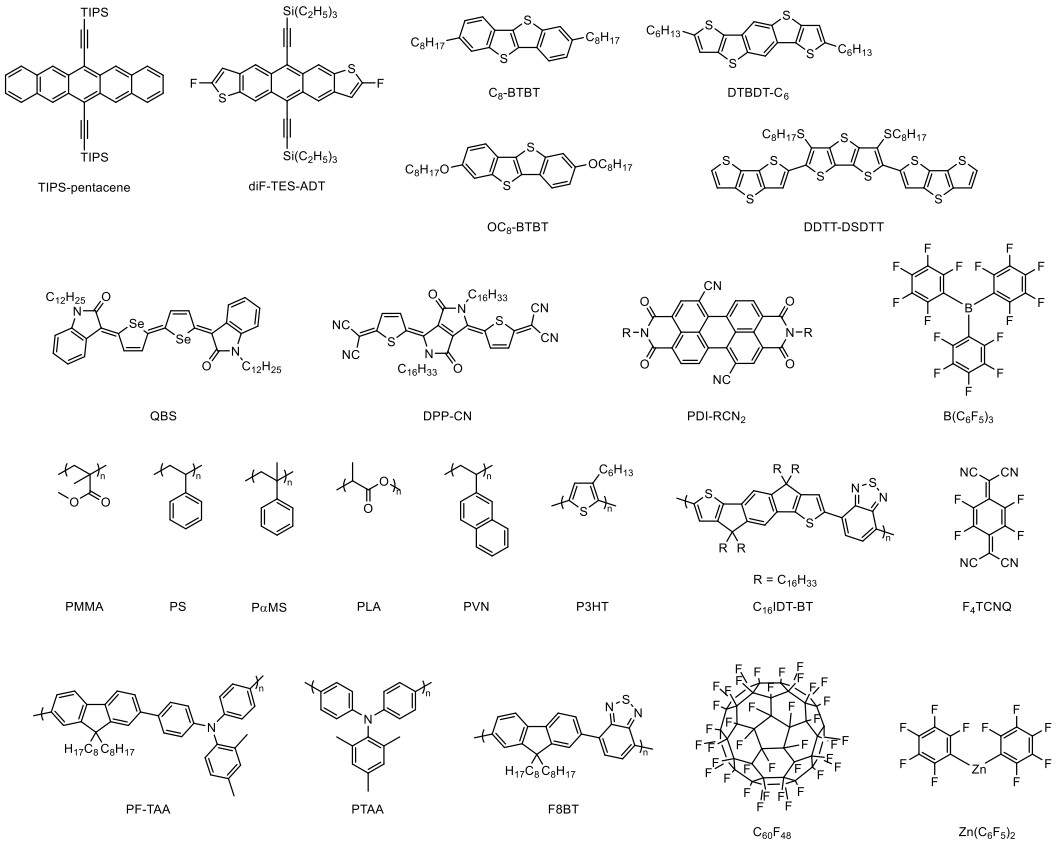

Figure 3 Examples of molecular semiconductors and polymers used in molecule:polymer blends.

The use of blends of small organic semiconducting molecules and organic polymers, which can be insulating as well as semiconducting, and possibly also dopants, offers an interesting alternative to the use of pristine small organic semiconductors. Techniques such as vacuum evaporation or single crystal growth are widely used to characterize the electrical properties of small molecules, but the given techniques are not very suitable for the formation of uniform thin films on large areas, and therefore do not meet the needs of mass semiconductor production. Incorporation of polymer binders allows the use of solution processing techniques such as drop-casting, spin-coating, inkjet printing and blade coating, and affects the crystallization ability and polymorphism of a small semiconductor molecule, thus ensuring the uniformity and reproducibility of the entire coated surface. The disadvantage of this technique, however, is the necessary solubility of all components and careful optimization of the selected polymer binder, its ratio with the semiconducting molecule and the deposition technique.

Blends of small molecules and polymers typically undergo phase separation, which strongly affects the microstructure and often leads to layered structures.[105] Similarly to the change of solvent during

crystallization, where we can observe a change in crystal structure, so the presence of a binding polymer can affect the morphology and microstructure, and thus the electronic properties of the small molecule in the resulting blend. Phase separation can be vertical or lateral. Lateral separation is undesirable because it destroys in-plane conductive pathways and its reduction can be achieved by reducing the surface energy of the substrate and reducing the rate of solvent evaporation.[105,106] Vertical separation, on the other hand, is desirable because it preserves and often improves the continuity, crystallinity, and packing of small molecules.[107] It takes place either by nucleation and growth of one component in the surrounding medium[108] or by the spinodal route, i.e. by exceeding the stability limit of the solution, which is separated into phases.[109] Vertical separation is controlled by Gibbs free energy, solvent evaporation kinetics, and solution/atmosphere, solution/substrate phase interactions.[106] In practice, it means changing the solvent (mixture of solvents), changing the binding polymer, its molecular weight and its ratio with the small molecule.[110–112] Investigating a specific blend and its phase separation, it is necessary to also consider the appropriate device structure (e.g. top- or bottom-gated transistor) for charge transport measurements depending on the vertical phase separation and in which part of the film the small molecule semiconductor will be located.

Due to its good monocrystalline properties, the soluble pentacene derivative 6,13-bis(triisopropylsilylethynyl)pentacene (**TIPS-pentacene**, Figure 3) has been subjected to intensive study of the properties of polymer blends. A common binding polymer for **TIPS-pentacene** is poly(methyl methacrylate) (**PMMA**, Figure 3). Deposited by a vertical flowing technique, this blend revealed that anisotropic crystalline growth occurred during vertical separation. As a result, the hole mobility of the layer was 0.3 cm^2/Vs (parallel direction) and 0.03 cm^2/Vs (perpendicular direction).[113] The same blend coated by electrostatic spray deposition from a mixture of o-dichlorobenzene and acetone showed better vertical separation and morphology when coating a small molecule:polymer mixture at once than layer by layer. The solvent vapor annealing also had a positive effect on the vertical separation and the given optimization improved the hole mobility from $2.2 \cdot 10^{-2}$ cm^2/Vs to $5.4 \cdot 10^{-2}$ cm^2/Vs.[114] The importance of the solvent has also been demonstrated for the given blend and coating technique. The use of o-dichlorobenzene did not lead to vertical separation due to the good solubility

of both components, which led to a hole mobility of $2.4 \cdot 10^{-2}$ cm^2/Vs. However, by using butyl acetate, the vertical separation led to the growth of larger crystalline domains than in case of the pristine material causing a much higher hole mobility of 0.88 cm^2/Vs.[115] Other binding polymers used along with **TIPS-pentacene** are poly(α-methylstyrene) (**PαMS**) and poly(triarylamine) (**PTAA**, Figure 3). Blends **TIPS-pentacene**:**PαMS** (1:1) and **TIPS-pentacene**:**PTAA** (1:1) spin-coated from tetralin yielded hole mobilities of 0.7 cm^2/Vs and 1.1 cm^2/Vs respectively.[116] **TIPS-pentacene**:**PαMS** also proved the importance of the coating technique, as the blade coating of this blend between plasma-treated electrodes created a device with much better crystallinity compared to drop-casting and spin-coating with a substantially higher hole mobility of 4.6 cm^2/Vs. Plasma-treated electrodes resulted in vertical separation into a bilayer whereas by treating the electrodes with pentafluorobenzenethiol (**PTBF**), the vertical separation led to the formation of a trilayer in which the crystalline semiconductor domains were smaller with spherulitic texture, leading to a rapid decrease in hole mobility.[117] The effect on crystallization using a mixture of two solvents in the spin coating technique was performed on a **TIPS-pentacene**:polystyrene (**PS**, Figure 3) blend in a 3:1 ratio. A transition from a needle-like crystal using a single solvent, to platelet crystals using a two-component solvent system was observed. Using a mixture of mesitylene and anisole, a hole mobility of up to 1.82 cm^2/Vs was achieved.[118] The aforementioned blend also proved to be greatly influenced by molecular weight of the binding polymer; it was found that a higher molecular weight of the polymer, together with a lower shearing speed, caused a higher proportion of ribbon-like morphology than spherulitic morphology. By optimizing the conditions, using a solution shearing technique from toluene, a hole mobility exceeding that of the pristine material was achieved (8.3 cm^2/Vs). However, drop-casting and inkjet printing have only achieved hole mobilities of 1.1 cm^2/Vs and 1.11 cm^2/Vs respectively.[119–121]

The structurally related material 2,8-difluoro-5,11-bis(triethylsilylethynyl)anthradithiophene (**diF-TES-ADT**, Figure 3) was also investigated very intensively, mainly due to its superior properties compared to **TIPS-pentacene** in the pristine state, which also promises better results in blends. The spin-coated material together with **PMMA**, **PαMS** (from chloroform) and **PS** (from 1,1,1,2-tetrachloroethane) in a ratio of 1:1 showed that the crystallinity of the material was preserved with

PMMA and **PαMS**, with hole mobilities of $1.21 \cdot 10^{-3}$ cm^2/Vs and $9.4 \cdot 10^{-2}$ cm^2/Vs respectively. However, in the case of **PS**, the crystallinity deteriorated with a hole mobility of $1.75 \cdot 10^{-4}$ cm^2/Vs.[122] The reason was the high tendency of **PS** to crystallize which prevented phase separation because the small molecule was kinetically locked in the **PS** layer. The blend **diF-TES-ADT**:**PαMS** also proved the ability to affect the stability of the device. Neat **diF-TES-ADT** suffers from low stability to UV-Vis radiation and the charge mobility drops rapidly during irradiation. However, the **diF-TES-ADT**:**PαMS** (1:1) blend did not show any degradation.[123] A marked improvement in charge mobility was again achieved by blade coating using a mixture of mesitylene:anisole (8:2) as a solvent. In the **diF-TES-ADT**:**PS** blend, the crystallinity was changed from ribbon-like to sheet-like type with a resulting hole mobility of 6.7 cm^2/Vs. It is also important to note that when using low molecular weight **PS**, there was not enough vertical separation which lead to significantly lower hole mobility, whereas using high molecular weight **PS**, a layer with long-range lateral crystallization was formed.[124] The use of semiconducting polymers has further demonstrated their additional interesting function. By using **PTAA** and poly(dialkyl-fluorene-*co*-dimethyl-triarylamine) (**PF-TAA**, Figure 3), which form conductive bridges between the crystalline domains of **diF-TES-ADT**, active layers spin-coated from tetralin afforded a hole mobility of 2.5 cm^2/Vs with **PTAA** and 5.5 cm^2/Vs with **PF-TAA**. In the presence of **PF-TAA**, the small molecule crystallized better, which caused a better in-plane ordering and therefore much higher hole mobility compared with **PTAA**.[125] Similar results were achieved in other studies using poly(triarylamine) (**PTAA**, Figure 3). Spin-coated **diF-TES-ADT**:**PTAA** (1:1) from tetralin showed a hole mobility of 2.12 cm^2/Vs and an on/off ratio of 10^6. Vertical phase separation showed a strong dependence on the spin-coater speed; at 300 rpm, a trilayer with the aforementioned mobility was formed, but as the speed increased, a bilayer was formed with decreasing hole mobility. At 5000 rpm, the hole mobility decreased to $7.5 \cdot 10^{-2}$ cm^2/Vs.[126] After treatment of the electrodes with oxygen plasma the mobility of the aforementioned blend was further increased to 2.47 cm^2/Vs.[127] The highest hole mobility value was obtained by doping said blend with $B(C_6F_5)_3$; spin-coating from 1,2-dichlorobenzene with a dopant quantity of 2.4 mol% led to a record hole mobility of 8 cm^2/Vs. The presence of dopant not only caused molecular doping, but also greatly affected the microstructure;

doped layers exhibited long-range molecular terracing whereas layers without dopant did not show this improved texture.[128]

Thiophene-based materials are also interesting candidates due to their good charge transport properties in the pristine state. One of the most studied small molecules is 2,7-dioctyl[1]benzothieno[3,2-b][1]benzothiophene (**C_8-BTBT**, Figure 3). Its blend with polylactide (**PLA**, Figure 3) inkjet-printed from chlorobenzene solution achieved a hole mobility of only $2 \cdot 10^{-3}$ cm^2/Vs, however, the ability of **C_8-BTBT**:**PLA** (10:1) to operate on a flexible membrane was demonstrated here, while pristine **C_8-BTBT** did not work under the given conditions.[129] Far superior results were obtained using indacenodithiophene-benzothiadiazole (**C_{16}IDT-BT**, Figure 3) as a polymer binder. The spin-coated blend **C_8-BTBT**:**C_{16}IDTBT** (1:4) from a mixture of tetralin and chlorobenzene (1:2) achieved a hole mobility of 1.4 cm^2/Vs. The addition of **$C_{60}F_{48}$** (Figure 3) as a dopant in a quantity of 1 mol% further increased the hole mobility to 7.8 cm^2/Vs. However, no dopant concentration affected the microstructure or vertical separation.[130] By changing the ratio of small molecule and polymer to 1:3, the lateral long-range crystallinity was improved in a given blend with 0.05 mol% **$B(C_6F_5)_3$** (spin-coated from 1,2-dichlorobenzene) with an achieved hole mobility of 11 cm^2/Vs.[128] A two-component solvent composed of tetralin and chlorobenzene 1:1 in a spin-coating of blend **C_8-BTBT**:**C_{16}IDTBT** (1:4) with **$C_{60}F_{48}$** (1 mol%) further increased the hole mobility to 13 cm^2/Vs,[131] and the blade coating of **C_8-BTBT**:**C_{16}IDTBT** (1:3) with the dopant **$C_{60}F_{48}$** (0.75 mol%) from the same solvent brought hole mobility to 14 cm^2/Vs. In addition to doping, the presence of dopant also affected the microstructure of the film, as improved in-plane crystallization was observed.[132] Spin-coating of the same blend from the same solvent doped by 0.025 mol% **$Zn(C_6F_5)_2$** resulted in a record hole mobility for the given blend (21.5 cm^2/Vs). The presence of the dopant was found to affect the microstructure, as the π-π stacking distance of the small molecule semiconductor was shortened.[133] Polystyrene was chosen as another polymer for the study of blends with **C_8-BTBT**. The importance of the ratio of small molecule to polymeric carrier was examined here, finding that ratios of small molecule and polymer close to 1:1 cause strong anisotropy in conductivity whereas ratios as high as 1:2 displayed much lower

anisotropy.[134] **C_8-BTBT**:**PS** (4:1 ratio) doped with 2,3,5,6-tetrafluoro-7,7,8,8-tetracyano-quinodimethane (**F_4-TCNQ**, Figure 3) coated by the bar-assisted meniscus shearing (BAMS) technique showed larger crystal domains compared to pristine material, with high crystalline quality and good connectivity between domain boundaries with a hole mobility of 10 cm^2/Vs. In a 4:1 ratio, the well-developed layer of small molecule was covered with a thin layer of **PS**. At a 1:2 ratio, however, the small molecule layer was undeveloped and non-uniform, causing a rapid drop in hole mobility. **F_4TCNQ** was used for doping contacts and without it, the given blend reached only a hole mobility of 1.5 cm^2/Vs.[135] For **C_8-BTBT**:**PS** blends deposited by the BAMS technique, it has also been proven that a thin top layer rich in **PS** prevents the diffusion of water and oxygen, thus increasing the stability of the device.[135] So far, the highest hole mobility value for this blend was achieved by the off-center spin-coating method. **C_8-BTBT**:**PS** (4:1) without dopant, spin-coated from *o*-dichlorobenzene, created a blend with a hole mobility value of 43 cm^2/Vs. The presence of the binding polymer caused the stabilization of the metastable (better organised) state of the small molecule with much better electronic properties.[136] A structural derivative of **C_8-BTBT** which also proved its function in small molecule:polymer blends is 2,7-dioctyloxy[1]benzothieno[3,2-b][1]benzothiophene (**OC_8-BTBT**, Figure 3), whose blend with **PS** (4:1), coated with the BAMS technique from chlorobenzene, showed a hole mobility of 0.92 cm^2/Vs and an excellent on/off ratio of 10^7. There was also a strong increase in the stability of devices where pristine material suffered from a decrease in a hole mobility, which fell by one order of magnitude after a year. However, the device using the blend retained a hole mobility of 0.3-0.6 cm^2/Vs even after 450 days.[137] Another fused thiophene material is 2,7-dihexyl-dithieno[2,3-d;2′,3′-d′] benzo[1,2-b;4,5-b′]dithiophene (**DTBDT-C_6**, Figure 3), which achieved a hole mobility of 1.00 cm^2/Vs (0.22 cm^2/Vs pristine) in a 4:1 blend with polystyrene inkjet-printed from toluene solution. In contrast to pristine material, no chasm at the grain boundary was seen in the blend.[138] A blend of 3',5'-bis(octylthio)-2,2':6',2''-terdithieno[3,2-b:2',3'-d]thiophene (**DDTT-DSDTT**, Figure 3):**PαMS** (1:1) deposited by solution shearing from anisole showed that the small molecule crystallizes into a nanoscale space in the polymer matrix, which ensures its better organization with a hole mobility of 2.44 cm^2/Vs.[139]

Also noteworthy is the blend of the entirely thiophene composition of **dH-PTTP** (Figure 1d, R = *n*-hexyl) and poly(3-hexylthiophene). **dH-PTTP**:**P3HT** (1:1) drop-casted from *p*-xylene only achieved a hole mobility of 0.1 cm^2/Vs, but in contrast to both pristine materials (**dH-PTTP** 0.002 cm^2/Vs, **P3HT** 0.01 cm^2/Vs), there was a tenfold improvement caused by the formation of conductive bridges between the large crystalline domains of **dH-PTTP** although the vertical separation in this case was negligible.[140]

To the best of our knowledge, so far there is only one system of small semiconducting molecule and polymer that shows ambipolar mobility. Quinoidal biselenophene (3Z,3'Z)-3,3'-((E)-5H,5'H-[2,2'-biselenophenylidene]-5,5'-diylidene)bis(1-dodecylindolin-2-one) (**QBS**):poly(2-vinylnaphthalene) (**PVN**), both depicted in Figure 3, in a 1:1 blend spin-coated from *o*-dichlorobenzene, compared to pristine material showed larger crystalline domains and reduced grain boundaries, resulting in hole and electron mobilities of 0.12 and 0.04 cm^2/Vs respectively.[141]

Blends of small molecules and n-type materials have not yet been studied as much as p-type materials. One of the few is 2,2′-[(2,5-dihexadecyl-3,6-dioxo-2,3,5,6-tetrahydropyrrolo[3,4-*c*]pyrrole-1,4-diylidene)dithiene-5,2-diylidene]dimalononitrile (**DPP-CN**, Figure 3):**PαMS** (1:1) spin-coated from tetralin, achieving an electron mobility of 0.5 cm^2/Vs, and due to enhanced stability, showing no signs of degradation during transistor operation in a normal atmosphere. In this case, we note the greatest improvement in properties using a blend, because it was not possible to create a functional transistor from the pristine small molecule, while with the help of a binding polymer a thin active layer with high and long-range uniformity was formed.[142] Apart from **DPP**, materials based on **PDI** were used in n-type small molecule:polymer blends. Despite the similar crystallinity of the pristine material (Figure 2) and its blend, **PDI8-CN_2**:**PS** (1:2) deposited by the BAMS technique reached an electron mobility of $2.8 \cdot 10^{-2}$ cm^2/Vs, whereas pristine material only $5.5 \cdot 10^{-3}$ cm^2/Vs. The ability of **PS** to encapsulate and protect the active layer from the atmosphere, which usually has a destructive effect on the electron transport, was observed here again.[143] Another representative of the n-type is the *N*,*N*-dialkyl-substituted-(1,7&1,6)-dicyanoperylene-3,4:9,10-bis(dicarboximide) derivative **PDI-RCN_2** (Figure 3) in a 1:1 blend with poly(9,9-dioctylfluorene-alt-benzothiadiazole) (**F8BT,** Figure 3), spin-coated from a mixed solvent of tetralin:chloroform (1:1). Compared to the pristine material, the macroscopic film

coverage and crystallinity of the n-type small molecule improved significantly, achieving an electron mobility of 0.25 cm^2/Vs (pristine 0.20 cm^2/Vs).[144]

3. Ionic interactions in small molecule semiconductors

A plethora of different interacting species can be considered in most organic electronic devices, whether they are nominally single active material devices such as transistors or compositionally more complex devices such as solar cells and bioelectronic sensors. In the context of charge transport, the neutral semiconductor as well as charged species such as polarons and bipolarons can potentially interact with omnipresent species such as oxygen and water.[64,145] While judicious control of the semiconductor's frontier energy levels and molecular structure can to some extent restrict unwanted side-reactions,[146,147] efforts are likewise placed on developing molecularly engineered additives that can minimize water- and oxygen-induced trap states.[148,149] Rather than circumventing intimate and potentially detrimental interactions between the organic semiconductor and ambient species such as oxygen and water, understanding, manipulating and taking advantage of these interactions – and extending them to encompass ionic species – can also be seen as the entry point to the world of organic bioelectronics. In the following, we will consequently survey and discuss the design of small molecule semiconductors for aqueous operation and intended interactions with biologically relevant ionic species.

3.1 Aqueous and non-specific ionic interactions

The bisphenylene-bithiophene-based p-type semiconductor **PTTP** discussed above is easily synthesized in a few steps from readily available starting materials, it is a bench-stable crystalline compound and it affords reliable OFETs whether the active layer is cast from solution or formed by thermal evaporation. As such, it is an obvious candidate for exploring chemical modifications and their impact on charge transport properties as well as ionic interactions. Considering first the introduction of an oxygen atom between the phenylene moiety and the alkyl chain, **dH-PTTP** was compared to the hexyloxy-analogue (**6O-PTTP**, Figure 4a) with the same approach taken with the longer C_8-chain (**dO-PTTP** *vs.* **8O-PTTP**).[150,151] Increased electron density caused by the mesomeric effect of the oxygen atoms resulted in a 0.15 eV decrease of the ionization potential for the alkoxy-derivatives compared to

the corresponding alkyl-derivatives, while solubility was also found to decrease markedly upon the introduction of oxygen. Only negligible differences in charge transport properties were found with and without the oxygen atoms; however, Sung *et al.* observed a nearly three-fold increase in hole mobility (0.065 cm^2/Vs *vs.* 0.18 cm^2/Vs) when going from **6O-PTTP** to **8O-PTTP**.[150] Increasing the polarity of the peripheral chain further and introducing a hydrogen bond donor, Katz and co-workers developed the hydroxy-terminated **6OH-PTTP**.[152] Although not examined for interaction with ionic species, it was found that bottom-gate top-contact OFET sensors comprising **6OH-PTTP** responded strongly to the phosphonate nerve agent model compound dimethyl methylphosphonate. Sensing behavior was also observed with **dH-PTTP**, but a bi-layer device configuration with a **dH-PTTP** bottom layer and a **dH-PTTP**:**6OH-PTTP** top layer afforded much improved response times while maintaining a high saturation current. The superior sensor performance with **6OH-PTTP** was ascribed to increased adsorption and subsequent diffusion of the analyte in the active layer due to hydrogen bond formation between the terminal hydroxy-groups and the polarized P=O bond in the phosphonate. It should be noted that the ubiquitous semiconducting polymer poly(3-hexylthiophene) (P3HT) has been modified with a similar side chain motif containing terminal hydroxy-groups incorporated at various percentages.[153,154] Although a low degree of aqueous swelling was observed, firm evidence from spectroelectrochemistry and OECT fabrication supports the fact that this polar motif facilitates ionic conduction in the bulk semiconductor film. Parr *et al.* took a step further and decorated **PTTP** with peripheral triethylene glycol (TEG) chains.[155] The electronic effect of the TEG chain was similar to that of the alkoxy, with a 0.12 V decrease of the first oxidative half-wave potential compared to **dH-PTTP**. Performing thin film cyclic voltammetry in an aqueous electrolyte, **TEG-PTTP** displayed much higher current densities than **dH-PTTP**, and a clear onset of oxidation congruent with much improved ionic conduction in the solid state was observed with the highly polar TEG chains as illustrated in Figure 4b. Comparing again **dH-PTTP** and **TEG-PTTP**, Guilbert *et al.* investigated in detail the impact of polar chains on structural properties as well as structural dynamics.[156] From single crystal X-ray diffraction analysis (Figure 4c), the thiophene-thiophene dihedral angle is in both compounds found to be 180 °(s-trans conformation) as expected with both compounds displaying a herringbone packing structure.

However, the thiophene-phenylene dihedral angle is significantly larger for **TEG-PTTP** (17.3 ° *vs.* 3.8 ° for **dH-PTTP**), most likely related to the markedly different chain conformations observed for the two compounds. Two gauche conformations are observed for each TEG chain, giving rise to the folded chain conformations,[157,158] whereas the hexyl chains exclusively show anti conformations and therefore the well-known zig-zag extended structure.

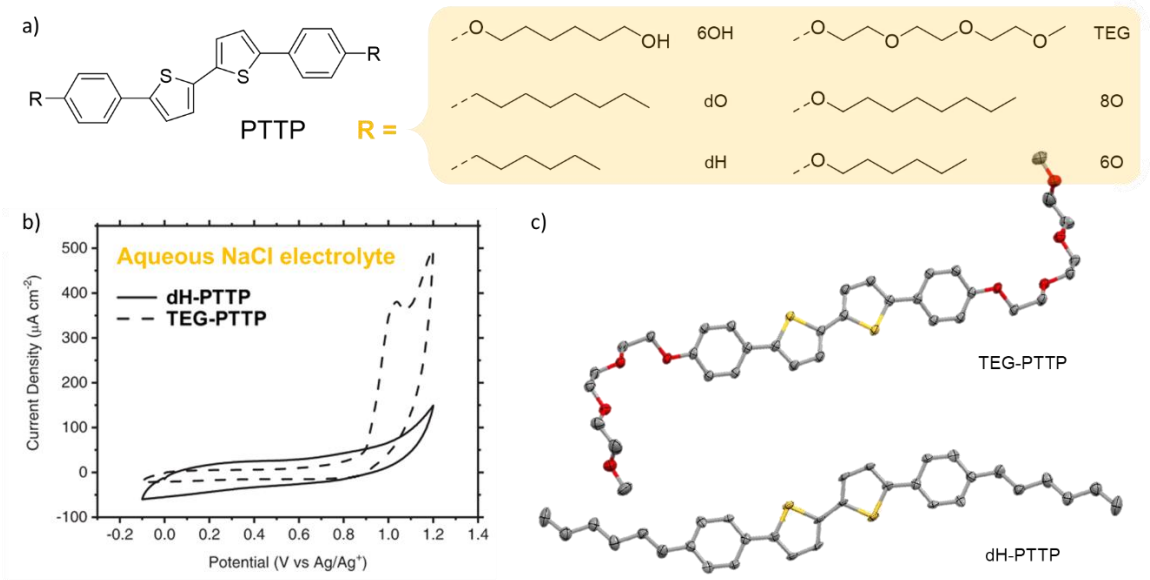

*Figure 4 Structure of **PTTP** and different peripheral substituents explored (a); cyclic voltammograms of **dH-PTTP** and **TEG-PTTP** thin films recorded in aqueous sodium chloride electrolyte (b, adapted from ref. [155]. Copyright 2020 Wiley under CC BY license https://creativecommons.org/licenses/by/4.0/); crystal structures of **TEG-PTTP** and **dH-PTTP** (c, data from The Cambridge Crystallographic Data Centre, CCDC 2052663 and CCDC 600832).*

Structurally related to **PTTP**, **DDFTTF** comprises a bithiophene core with fluorene moieties replacing the phenylene units and peripheral *n*-dodecyl solubilizing chains.[159] Using a cross-linked poly(4-vinylphenol) dielectric layer with high stability towards air and moisture, Bao and co-workers fabricated **DDFTTF**-based OFETs that could be operated efficiently in an aqueous environment. With high hole mobilities around 0.3 cm^2/Vs at low gate bias (< 1 V), the devices showed negligible degradation even after 10^4 cycles while exposed to water. Subsequent work incorporating **DDFTTF** into a transistor made from biodegradable substrate (poly (L-lactide-co-glycolide)) and dielectric (poly(vinyl alcohol)) is paving the way for fully biocompatible and biodegradable electronic devices.[160]

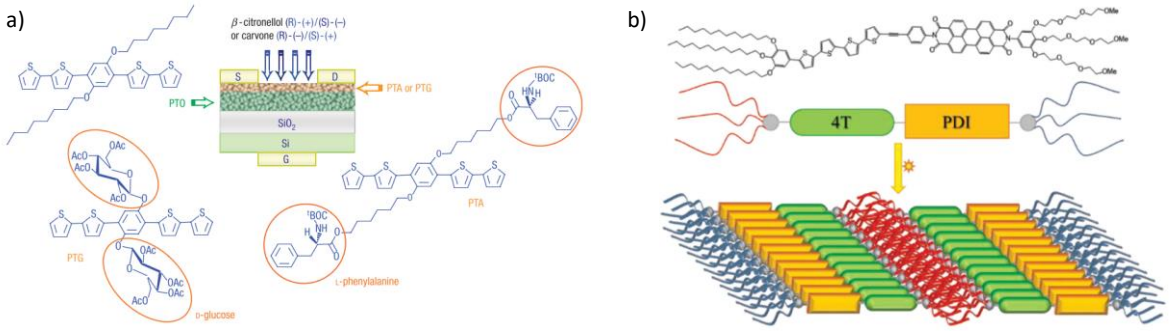

Figure 5 Sensing platform for differentiation of chiral analytes (a, reproduced with permission from ref. [161]*. Copyright 2008 Nature Publishing Group); humidity sensor from supramolecular organization of amphiphilic donor-acceptor dyad (b, reproduced with permission from ref.* [162]*. Copyright 2015 Wiley).*

Using a related bi-layer structure to the one described above for **6OH-PTTP**, Torsi *et al.* used the alkoxyphenylene-thiophene semiconductor **PTO** depicted in Figure 5a as a bottom transport layer and a chemically modified sensing layer on top.[161] By covalent attachment of the chiral recognition units D-glucose (**PTG**) or L-phenylalanine (**PTA**) to the small molecule semiconductor, the resulting bi-layer OFET sensors were able to differentiate between the chiral natural products (R)-(−)- and (S)-(+)-carvone and (R)-(+)- and (S)-(−)-β-citronellol, respectively. This proof-of-principle study was carried out with neat analyte vapors in a nitrogen atmosphere. Analyte molecules are consequently hypothesized to diffuse into the semiconductor film along grain boundaries and eventually reach the semiconductor/dielectric interface where physisorption will modulate the current. The top sensing layer, due to its chiral recognition elements, will interact preferentially with one isomer, thus slowing its diffusion and thereby giving rise to the eventual differentiation between optical isomers.

General design criteria for molecular engineering of small molecule semiconductors to create designated channels or pathways for ionic conduction are far from being firmly established yet. Nevertheless, Squillaci *et al.* found the amphiphilic small molecule donor-acceptor dyad **4T-PDI** shown in Figure 5b to self-assemble into a highly ordered supramolecular structure characterized by an aliphatic core and strong π-π interactions between neighboring quaterthiophene segments and between neighboring perylene diimide segments as well.[162] Further macroscopic organization into nanoribbons that subsequently bundle together into long one-dimensional fibers with exposed hydrophilic TEG chains was exploited to fabricate resistive humidity sensors with fast responses and

high sensitivities. In a follow-up study, a simpler bolaamphiphilic structure with a sexithiophene core was used in a similar manner to create one-dimensional fibers that can be used to fabricate electrical resistive humidity sensors.[163]

3.2 Ion-selective interactions

Ion specific interactions of organic materials with inorganic ions in the form of various moieties including crown ethers, calixarenes, rotaxanes and other supramolecules have been well reported for many decades for many applications, from spectroscopic sensing molecules to ion chelation in waste and catalysis.[164] Indeed, much excellent science has been reported over the years and supramolecular chemistry constitutes an expansive topic well beyond the scope of this review. We will therefore limit the discussion to ion specific interactions with those materials which might be familiar to the organic semiconductor community.

Introduction of ion selectivity into polythiophene has been achieved via introduction of a oligoether bridged bithiophene unit whereby 2,2”-bithiophene is functionalized at 3- and 3”-positions with n-ethylene glycol bridge, where n = 3 or 4 which binds Na^+ and K^+ selectively, respectively (**M-Na**$^+$ and **M-K**$^+$, see Figure 6a).[165] The ionochromism displayed by this system relies on the planar conformation of the bithiophene unit which, when binding an alkali metal ion to the oligoether bridge, undergoes a backbone twist along the thiophene-thiophene bond, reducing the overlap of the π-bonding orbitals and thus reducing conjugation length and causing a blue shift in the observed color of the material. The authors reported both Na^+ and K^+ selective copolymers with **M-Na**$^+$ and **M-K**$^+$ monomers respectively, which exhibit an ionochromic response of up to 90 nm in absorption spectroscopy. The backbone twist of the parent bithiophene has since been examined by X-ray crystallography both as molecules and complexes.[166] Upon complexation of Na^+ by the **M-Na**$^+$ molecule, the S-C-C-S dihedral angle of the parent bithiophene is twisted from 3.2 ° in the unbound form to 75.9 °, and the **M-K**$^+$ molecule is likewise twisted from 14.0 ° to 84.6 ° as a result of metal ion binding. When copolymerized with benzo[1,2:4,5-*b*′]dithiophene monomers with both alkyl and oligoether side chains, the authors report ionochromic copolymers with a solution-phase colourimetric response with a λ_{max} shift of 40-70 nm. It should be noted in both these cases that the lower initial planarity of the **M-K**$^+$ monomer results

in a smaller shift in λ_{max}. The polymers also displayed promising solid state ionochromism and a shift of approximately 20 nm in the photoluminescence spectrum upon binding of Na^+ and K^+. Small molecule chromoionophores containing the **M-Na$^+$** ionophore have been synthesized.[167] A series of tetra-aryl molecules were synthesized with increasingly electron withdrawing endcaps, with moderate to high ionochromic response in solution phase to Na^+ and with high selectivity to Na^+ over Li^+, K^+ and Ca^+. The molecules exhibit a low limit of detection across the visible spectrum. Dual fluoro- and chromoionophores have also been synthesized according to a similar method with both **M-Na$^+$** and **M-K$^+$**.[168] The authors demonstrated both ratiometric and fluorimetric sensing of both Na^+ and K^+ alongside the well-reported ionochromic response. Utilizing the tunability of the optoelectronic properties of conjugated materials, the authors demonstrate a bimolecular Na^+/K^+ sensing system with a discrete colorimetric response to Na^+ or K^+ or both in solution. By selecting the peripheral π-conjugated moiety carefully, the authors show fluorimetric turn-on, turn-off and ratiometric response to the presence Na^+ or K^+ ions in solution phase in polar organic solvents as exemplified in Figure 6b. The fluorimetric response could be modulated from turn-off to turn-on to ratiometric, corresponding to the donor or acceptor character of the peripheral moiety. All donor systems based on a sexithiophene backbone afforded a turn-off fluorimetric response. Strong acceptor moieties based on 2,1,3-benzothiadiazole afforded turn-on fluorescence, and weak acceptor moieties based on tetrafluorophenylene moieties afforded a ratiometric response. In all examples of the bithiophene-based crown ether systems, lower binding constants of the **M-Na$^+$** and **M-K$^+$** for Na^+ and K^+ respectively were observed than the parent crown ethers in competitive binding experiments.

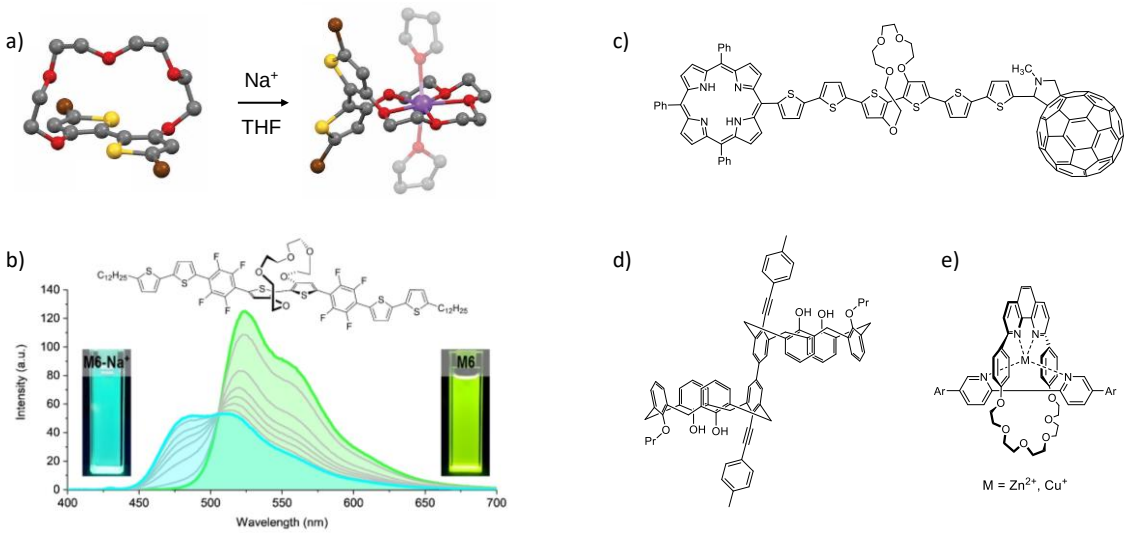

Figure 6 Functionalized bithiophene moiety for alkali metal ion binding (a, image reproduced from ref. [166]. Copyright 2016 Wiley under CC BY license https://creativecommons.org/licenses/by/4.0/); ratiometric fluorimetric sensing of sodium ions (b, image reproduced from ref. [168]. Copyright 2020 Royal Society of Chemistry under CC BY license https://creativecommons.org/licenses/by/4.0/); complexation-gated molecular wire for intramolecular photoinduced electron transfer (c); calixarene-based nitric oxide sensor (d); rotaxane-based Zn^{2+} and Cu^{+} sensor (e).

The **M-Na**$^{+}$ system has been employed as a molecular switch in a molecular wire.[169] A porphyrin ring and C_{60} fullerene were employed to end-functionalize a sexithiophene moiety containing a central **M-Na**$^{+}$ unit (Figure 6c). In the non-complexed form, photoexcitation of the porphyrin ring is followed by electron transfer through the thiophene bridge to the C_{60} fullerene, as demonstrated with characteristic transient absorption spectra transitions for C_{60} and sexithiophene. Upon Na^{+} complexation, the electron transfer through the molecule cannot occur, with transient absorption spectroscopy showing transitions characteristic of porphyrin only. Extension of this type of system in small molecules has been attempted, though examples are few. A similar terthiophene bridged type system has been employed as a Pb^{2+} sensor with a mixed crown ether containing both sulfur and oxygen atoms.[170] Compared to the bithiophene system, this molecule is somewhat less effective, giving a much smaller shift in the absorbance spectrum as a result of the central 3,4-ethylenedioxythiophene (**EDOT**) unit contributing to the planarity of the molecule in both the non-complexed and complexed forms.

Complexation of Pb^{+} has a significant effect on the electrochemistry, contributing to a marked increase in ionization potential.

Crown ether moieties have been employed as pendant groups in small molecule systems for ion selective interaction. Rylene diimide dyes have been well-explored for their relatively simple *N*-alkylation with crown ether moieties. A barium sensor was synthesized based on naphthalene diimide (**NDI**) alkylated at the terminal nitrogen atoms with 15-crown-5 complexes. The crown ether-functionalized **NDI** is capable of binding selectively with barium ions. When exposed to Ba^{2+}, a bimolecular sandwich complex of two **NDI** moieties and two barium ions coordinated by the crown ether moieties is formed. This complex forms an intermolecular excimer, a pseudo-energy level created by the π-stacked **NDI** moieties, which has fluorescence emission at 450 nm. This process is selective for Ba^{2+} over K^{+}. The authors suggest that this selectivity is due to the formation of a more stable complex of **NDI-Ba^{2+}** than **NDI-K^{+}**.[171] A similar perylene diimide system (**PDI**), functionalized at the perylene aromatic core with a 15-crown-5 moieties, conversely displays a fluorescence turn-off in the presence of barium ions and demonstrated selectivity to Ba^{2+} over a number of other alkali metal cations forming similar self-assemblies to the **NDI** based systems.[172] Zinc sensors employing **NDI** have also been demonstrated.[173] Employing a zinc-selective ligand to functionalize the core, the authors demonstrated a fluorescence turn-on sensor selective to **NDI**.

Selector *et al.* synthesized two oligothiophenes functionalized with a benzo-15-crown-5 located at either the 5- and 5’’- or 3- and 3” positions of the terminal thiophenes.[174] The two structural isomers displayed marked differences in optoelectronic properties, and the supramolecular assemblies formed by these materials. The linear 5- 5’’-isomer is blue shifted in UV-Vis absorption spectrum by 100 nm compared to the 3,3’’-isomer. Upon formation of a film at the air-water interface, the 5,5’’-isomer formed a predominantly H-aggregate structure whereas the 3,3’’-isomer predominantly forms J-aggregates in the solid state. The structural isomers formed different complexes when exposed to Ba^{2+} ions. The 5,5’’-isomer formed a sandwich complex consisting of two Ba^{2+} ions coordinated between two molecules whereas the 3,3’’-isomer contorted to form a single-molecule-single-ion species in solution.

Certain calixarene species have been included in small molecules and subsequently polymers as the ion-interacting moieties. Calixarenes, generally, have a wide range of molecular, supramolecular and ion-specific interactions based on ring size and functionality. By functionalizing one of the benzene rings of 5,5′-bicalixarene, Molad *et al*. demonstrated conjugated fluorescence sensors incorporating the calixarene sensing moiety directly into the conjugated molecular backbone of molecules and polymers as illustrated in Figure 6d.[175] The molecules and polymer displayed a fluorescence quenching response to nitric oxide. Though not strictly an ion, the system could easily be adapted for specific sensing from the well-known supramolecular chemistry literature with the broad range of semiconductor building blocks to expand the range of ion-selective small molecular structures, and is worth noting here. Supramolecular chemistry based on rotaxanes has also been employed to confer ion interaction and selectivity onto small molecular systems, and subsequently polymeric systems.[176] In this case, 2,2'-bipyridyl functionalized at the 5- and 5'-positions with bithiophene, **EDOT** or **bisEDOT** could be complexed with Zn^{2+} or Cu^{+} and a phenanthroline based macrocycle (Figure 6e), resulting in a marked bathochromic and specific shift in UV-Vis absorption dependent on the complexed metal species. Although synthetically complex, these systems are good candidates for inclusion as it is likely that a very low loading of a polymeric or small molecule matrix with ion-selective species would yield a marked effect on physical properties.

Derivatization of fullerenes with crown ether moieties has been employed as a means to confer selective ion interaction and modulate solid state properties. In an effort to enhance cathode buffer layer performance and thus improve overall organic solar cell performance (OSC), Zhao *et al*. functionalized **PCBM** with a pendant 18-crown-6 potassium ion-selective moiety.[177] The authors employed the modified **PCBM** as a buffer layer between the ZnO cathode and the **PCBM**:**PTB7-Th** bulk heterojunction active layer. Their optimized device employed the potassium-doped fullerene system as a buffer layer between the solar cell cathode and the OSC. This system exhibited improved interfacial contact between the cathode and the organic semiconductor layer and interfacial charge recombination was reduced. The optimized device displayed a higher short circuit voltage and fill factor and an

enhanced solar cell performance, up from 8.4 % in their control system to 10.3 % in the ion-doped cathode buffer layer system.

In an effort to mimic lipid bilayer ion channel systems, Chen *et al.* functionalized C_{60} with twelve crown ethers of varying ring size to allow transport of Li^+, Na^+, K^+, Rb^+ and Cs^+ with various alkyl chain linker lengths connecting crown ether and C_{60} fullerene.[178] They explored the ability of their fullerene system as an effective method to transport ions across a lipid bilayer by fluorescence spectroscopic observation of the associated proton flux by a pH sensitive fluorophore into model vesicles. The ion transport into the vesicle was selective to the ion with the associated crown ether. The ion transport also exhibited a dependence on alkyl chain linker length which did not correlate with size of the alkali metal ion.

4. Mixed ionic and electronic conduction in small molecule semiconductors

It has already been firmly established that a plethora of small molecule semiconductors display very efficient electronic conduction when probed as the active material in an OFET configuration. From the discussion above, it is clear that organic semiconductors can also be modified to interact favorably with ionic species, while several systems are able to maintain their electroactive properties in an aqueous environment. This raises the question of whether small molecule semiconductors can be designed to display *both* ionic and electronic conduction without one detrimentally affecting the other, and thus be used as OMIECs for instance in OECT applications and more widely in bioelectronic devices.

Whereas electronic charge transport, as discussed in detail above, relies on a high degree of structural order to facilitate strong intermolecular interactions and efficient charge delocalization, ionic charge transport hinges on different prerequisites. Ionic transport in organic semiconductor films, in particular of hydrated ions originating from an aqueous interface as most relevant for bioelectronic applications, relies on ions first penetrating the semiconductor film and subsequently moving freely within the free volume of the semiconductor film. This indicates that ion transport is strongly dependent on the hydrophobicity of the semiconductor surface, with typically alkylated

systems providing a significant barrier for ion injection into the film.[27] The microstructure of the semiconductor film is also important with a higher degree of porosity and/or disorder being beneficial for ion transport within the bulk semiconductor material.[179] Due to the often direct interface between the semiconductor and an aqueous environment, the water uptake and its impact on the semiconductor microstructure also plays a crucial role.[180,181] In this context, swelling provides more pathways for ionic transport but can on the other hand be detrimental to the electronic charge transport due to the swelling-induced structural disorder. This highlights the often opposing design criteria for optimizing ionic and electronic transport and how this must frequently be approached as a delicate balancing act.

The electrochromic behavior of many semiconductor systems has enabled direct measurement of ion transport by electrochromic moving front experiments that can be monitored optically in a straightforward manner.[182,183] Mixed ionic and electronic conduction, meanwhile, can be assessed using the organic electrochemical transistor (OECT) mentioned briefly in the introduction. Similar to an OFET, the OECT is a three-electrode transistor with the semiconductor sandwiched between two source and drain metal electrodes. Contrary to an OFET, gating takes places using a gate electrode immersed in an electrolyte that is directly interfaced with the semiconductor. As such, electronic charge transport from source to drain electrode is modulated by electrochemical doping (or dedoping) of the bulk semiconductor film. To compensate the accumulation (or depletion) of electronic charges, ions of opposite charge move into (or out of) the film upon gating. While charge accumulation and transport takes place near the semiconductor-dielectric interface in an OFET as well as in an electrolyte-gated OFET, true OECT operation is accompanied by volumetric doping and dedoping which emphasizes the coupling between electronic and ionic transport.[184] Among the OECT device characteristics, the transconductance (ideally normalized by active layer thickness) describes the sensing capabilities of the device, while the μC* product is the device figure-of-merit that is used to evaluate the combination of electronic charge carrier mobility (μ) and volumetric charge storage capacity (C*) in an OMIEC.[185]

Following on from the initial work with **TEG-PTTP** (Figure 4), which could be oxidized electrochemically as a thin film in aqueous electrolyte, Parr *et al.* sought to explore this conjugated

motif further in the context of mixed ionic and electronic conduction.[155] Motivated by a relatively high onset of oxidation and an irreversible electrochemical process for **TEG-PTTP**, the two central thiophene moieties were substituted for the more electron-rich **EDOT** moieties. Compared to **TEG-PTTP**, the **bisEDOT**-derivative **P2E2** (Figure 7a) displayed a markedly lower onset of oxidation (0.34 V *vs.* 0.93 V measured versus the Ag/Ag^+ redox couple) while also showing much more reversible oxidative electrochemical behavior in aqueous electrolyte as seen in Figure 7b. Doubling the length of the aromatic core afforded the related molecule **P4E4** (Figure 7a), comprising four central **EDOT** units and two peripheral phenylene units on either side, again terminated by TEG chains.[155] A further lowering of the onset of oxidation (0.22 V *vs.* Ag/Ag^+) was observed for a thin film of **P4E4** in aqueous electrolyte, while the cyclic voltammogram depicted in Figure 7c now displayed two distinct oxidative processes ascribed to initial generation of the radical cation followed by subsequent dication formation. Spectroelectrochemical studies of **P2E2** and **P4E4** thin films confirmed that bulk electrochemical doping takes place with complete bleaching of the π-π* absorption band and concurrent appearance of spectral features from the oxidized species with applied bias. This has previously been established as a prerequisite for efficient OECT materials.[23] Nevertheless, only **P4E4** was successfully employed as the active material in an OECT; the lack of current modulation with **P2E2** was attributed to an unfavorable packing in the solid state with limited pathways for intermolecular charge transport. The **P4E4**-based OECTs turned on at low gate bias, albeit displaying low currents in the nA range and significant hysteresis. A boost in OECT performance with currents in the 100 nA range and significantly reduced hysteretic behavior was found when blending polyethylene oxide (**PEO**) into the active layer. A μC* product, widely adopted as one of the main figures-of-merit for OECTs, of 0.81 F V^{-1} cm^{-1} s^{-1} was achieved for **P4E4** with 10 wt% high molecular weight **PEO**. The improved performance with **PEO** was corroborated by higher current densities in the cyclic voltammogram and a higher ion diffusion coefficient measured by variable scan rate cyclic voltammetry.

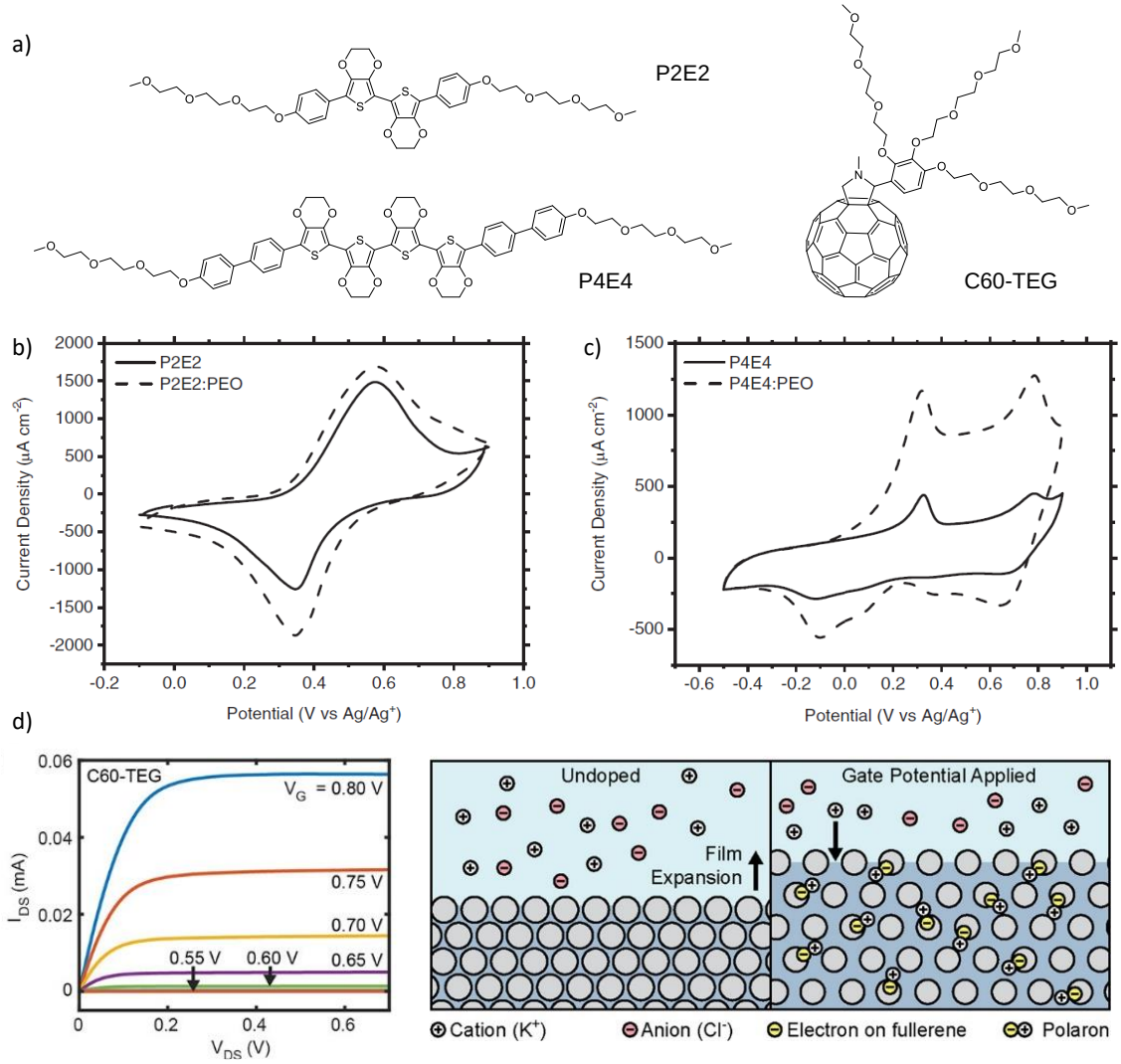

*Figure 7 Structures of organic mixed ionic and electronic conductors (a); cyclic voltammograms of **P2E2** (b) and **P4E4** (c) thin films with and without PEO additive recorded in aqueous sodium chloride electrolyte. Graphs reproduced from ref.* [155]. *Copyright 2020 Wiley under CC BY license https://creativecommons.org/licenses/by/4.0/; OECT output curves and schematic illustrating the ionic interactions and film expansion for **C60-TEG** upon doping (d, images reproduced from ACS Appl. Mater. Interfaces 2019, 11, 28138−28144. Copyright 2019 American Chemical Society).*

Focusing instead on n-type OECT operation, Bischak and co-workers turned their attention to fullerene derivatives, which are well-established electron transport materials in the wider organic electronics community as discussed above. Comparing the archetypical fullerene derivative **PCBM** with the hydrophilic **C60-TEG** derivative decorated with three TEG chains (Figure 7a), the latter was found to work as an efficient OMIEC when probed as the active material in an OECT configuration.[186] Spin-coated films of **C60-TEG** with thicknesses ranging from 60 to 150 nm afforded n-type OECTs with a threshold voltage around 0.56 V and currents in the μA regime when gated up to 0.8 V (Figure 7d), with higher bias inducing device degradation. A transconductance value of 4.1

μS was reported at 0.8 V (for a device with active layer dimensions W = 400 μm, L = 20 μm, and d = 140 nm) and a μC* product of 7.0 F V^{-1} cm^{-1} s^{-1} was extracted from a series of devices with varying transistor dimensions and film thicknesses. Spectroelectrochemical measurements again confirmed that bulk electrochemical doping takes place with **C60-TEG** thin films in aqueous electrolyte, contrary to the case for the hydrophobic analogue **PCBM**. An electrochemical quartz crystal microbalance was furthermore used in conjunction with atomic force microscopy to monitor changes in mass and thickness of the two fullerenes upon electrochemical doping. In agreement with previous work on hydrophilic and hydrophobic polythiophenes,[27] the hydrophilic **C60-TEG** was found to swell due to water and ion uptake while **PCBM** remained unaffected. The onset of swelling coincided with the onset of electrochemical doping and the mass uptake was dominated by cations compensating the negative polarons formed upon doping as illustrated in Figure 7d.

5. Conclusion and Outlook

Small molecule semiconductors can be designed to show excellent charge carrier mobilities in transistor configurations and a wide array of different molecular classes comprising conjugated aromatic rings, extended fused aromatic systems, and quinoidal structures highlight the richness of the chemistry toolbox that is available for molecular design. Moreover, access to both electron-rich and highly electron-deficient building blocks enables both p-type and n-type charge transport. Compared to semiconducting polymers, small molecule semiconductors can be harder to process into continuous thin films using scalable methods, and many molecular systems are more sensitive to processing conditions with subtle variations in extreme cases giving rise to differences in performance of the order of several magnitudes. Yet, being able to study systems ranging from single crystal transistor devices to blends of molecular semiconductors with insulating binder polymers also highlights the many opportunities and vast parameter space available for studying molecular semiconductors and developing them further for new applications such as those relying on mixed ionic and electronic conduction discussed herein.

Work on semiconducting polymers for OECT applications has highlighted the oligoethylene glycol chain as a suitable hydrophilic motif that can facilitate ionic conduction in the bulk

semiconductor film. For several polymeric systems, both p- and n-type, it has now been shown that substituting archetypical alkyl chains for oligoethylene glycol chains will shift the semiconductor operation from an OFET to an OECT regime due to this bulk ionic conduction which enables volumetric doping by compensating the charged semiconductor.[24,187] So far, the work on small molecule semiconductors for OECT applications has followed these molecular design criteria closely with both p- and n-type small molecule OECT materials bearing triethylene glycol chains.[155,186] Meanwhile, detailed studies have been devoted to a deeper understanding of the intricate interplay between electronic and ionic conduction and the driving forces for ion movement in and out of the semiconducting film during OECT operation.[188–191] Work so far on small molecule semiconductors indicate a similar mode of operation compared to polymeric systems with ion movement in and out of the semiconductor film closely following the electrochemical doping and dedoping processes.[186] While positives can be taken from the fact that the oligoethylene glycol motif has been established as a reliable means for enabling bulk ionic conduction, further exploration of other motifs from within the synthetic chemistry community is likely to help the continued development of OMIECs. For instance, p- and n-type OECT operation requires the influx of negatively and positively charged ions, respectively, for charge compensation and we imagine that different "ion-transporting" motifs are likely to be ideal for the two scenarios. It is also worth noting that a material like poly(benzimidazobenzophenanthroline) (**BBL**), which completely lacks hydrophilic chains, shows excellent n-type OECT performance.[192,193] Reducing or as in the case of **BBL** completely eliminating the proportion of hydrophilic chains relative to the π-conjugated backbone will help to increase the charge storage capacity and therefore the μC* product.

As we have highlighted herein, molecular engineering of small molecule semiconductors is a delicate act where subtle chemical modifications can disrupt the molecular packing easily and consequently the charge transport properties. Not only can these chemical modifications lead to a different crystal packing, even small molecular displacements and changes in energetic disorder in a given crystal system can give rise to large changes in charge transport properties. Therefore, further work is needed to explore more systematically the impact of chemical modification on molecular

semiconductors and to identify π-conjugated systems that are particularly resilient to these modifications.[194,195] We envision potential directions for this work also to include investigations into polar motifs with more structural similarity to the simple alkyl chain than for example oligoethylene glycol chains which show a preference for the gauche conformation resulting in significantly different structural organisation.[155,156] Alkyl chains with terminal hydroxy groups represent one such example, explored previously on a polythiophene scaffold with good mixed ionic and electronic conduction behavior despite a very low degree of swelling in aqueous electrolyte compared to glycolated analogues.[154] Polar motifs that can help guide the structural organization, for instance through intermolecular hydrogen bonding as known from self-healing organic semiconductors,[196] is another avenue that invites further studies. So-called hybrid chains, comprising both hydrophilic and hydrophobic segments, are likewise worth exploring for molecular semiconductors with a view to separate the ionic and electronic pathways and thus limit coulombic charge trapping.[197] Self-doped systems, explored for OECTs already in the form of conjugated polyelectrolytes,[198,199] present another potential direction for small molecule OMIECs. Finally, as machine learning approaches and predictive calculations of material structure and properties are becoming increasingly advanced,[200,201] computational methods should be considered alongside experimental discovery.

Taking inspiration from high-performing OFET materials and exploring similar structural motifs for OECT applications does come with some caveats and limitations. In addition to the restrictions governed by the electrochemical window of the aqueous electrolyte, efforts to identify p- and n-type OECT materials with low ionization and reduction potentials, respectively, are also motivated by a desire to prevent unwanted side reactions and degradation of the active material at excessive electrochemical potentials. This places a strong emphasis on identifying sufficiently electron-rich and –deficient materials for OECTs. In polymeric semiconductors, significant lowering of ionization potentials can be achieved for instance by substituting 3-alkylthiophenes with 3-alkoxythiophene motifs; the relatively high side chain density of many polythiophenes means that the cumulative effect from the mesomerically electron-donating alkoxy substituents is rather large (on the order of 0.5 eV).[27,202] In small molecule semiconductors, on the other hand, limited sites for

functionalization are often available. The extended fused aromatic systems such as **BTBT** (Figure 1) and **DNTT**, for instance, have relatively large ionization potentials with only the peripheral positions accessible for chemical modification. Comparing **dH-PTTP** and **TEG-PTTP** (Figure 4a) illustrates the limited influence of the mesomeric effect in small molecule systems with peripheral substituents with only a 0.12 V shift in the first oxidative half-wave potential when going from hexyl to TEG substituents.[155] Despite excellent charge transport properties, straightforward repurposing of fused aromatic systems for OECT applications consequently seems challenging if the frontier energy levels are not already compatible with stable and reversible aqueous operation. Countering the argument for p-type materials with very low ionisation potentials, it is important to also keep in mind potential side reactions with ambient species such as molecular oxygen during OECT operation.[147]

While the crystallinity of small molecule semiconductors poses a potential obstacle in terms of identifying ion-transporting moieties compatible with a favorable structural organization it also offers potential benefits. Mechanistic studies often hinge on detailed structural and spectroscopic studies, preferably performed in operando to understand the interplay between ionic and electronic transport,[191] and it is conceivable that an efficient and highly crystalline small molecule system could offer unprecedented insight into the mechanisms of mixed ionic and electronic conduction. As discussed herein, small molecule semiconductors lend themselves very well to blending with both insulating and semiconducting polymers. This approach could be very promising for bioelectronic applications; a lower degree of interdependency between the ionic and electronic conduction could potentially be achieved using a blend of an ionic conductor and an electronic conductor. Moreover, this approach can in principle be explored with commercially available materials surpassing the need for often labor- and time-consuming synthesis and purification of new materials. A similar argument can be made for work on non-aqueous devices, exemplified by electrochemical doping of conventional polymeric semiconductors through ionic liquids or aqueous-organic liquid-liquid interfaces.[203,204] These approaches can likewise be pursued for small molecule semiconductors in attempts to reap the benefits of the very high charge carrier mobilities seen in small molecule systems.

Having highlighted herein a number of ion-specific interactions in molecular semiconductors, we emphasize the potential for this class of materials to advance work on ion-selective bioelectronic devices.[205–207] Although challenging, identifying and optimizing suitable ion-selective small molecule semiconductors for OECT operation could potentially lead to highly selective ion-sensing with all the required functionalities built directly in to the active material thus avoiding further device engineering.

In conclusion, we believe that the future is bright for small molecule mixed ionic and electronic conductors with a wide range of different research directions to explore. The interdisciplinary nature of this research means that contributions from theoretical and synthetic chemists alongside materials scientists, device engineers and physicists are all required to fulfil the great potential of this class of materials. Relying heavily on all the accumulated knowledge from the field of organic electronics is undoubtedly beneficial, but we should also look for inspiration from further afield given the many areas of chemistry and materials research that deal with ionic transport.

6. Acknowledgements

We gratefully acknowledge support from the Academy of Medical Sciences & Wellcome Trust (SBF002/1158) and the Materials Research Institute.

7. References

(1) Bronstein, H.; Nielsen, C. B.; Schroeder, B. C.; McCulloch, I. The Role of Chemical Design in the Performance of Organic Semiconductors. *Nat. Rev. Chem.* **2020**, *4*, 66–77

(2) Tang, C. W.; Vanslyke, S. A. Organic Electroluminescent Diodes. *Appl. Phys. Lett.* **1987**, *51*, 913–915

(3) Burroughes, J. H.; Bradley, D. D. C.; Brown, A. R.; Marks, R. N.; Mackay, K.; Friend, R. H.; Burns, P. L.; Holmes, A. B. Light-Emitting Diodes Based on Conjugated Polymers. *Nature* **1990**, *347*, 539–541

(4) Sariciftci, N. S.; Smilowitz, L.; Heeger, A. J.; Wudl, F. Photoinduced Electron Transfer from a Conducting Polymer to Buckminsterfullerene. *Science* **1992**, *258*, 1474–1476

(5) Yu, G.; Gao, J.; Hummelen, J. C.; Wudl, F.; Heeger, A. J. Polymer Photovoltaic Cells: Enhanced Efficiencies via a Network of Internal Donor-Acceptor Heterojunctions. *Science* **1995**, *270*, 1789–1791

(6) Sirringhaus, H. 25th Anniversary Article: Organic Field-Effect Transistors: The Path beyond Amorphous Silicon. *Adv. Mater.* **2014**, *26*, 1319–1335

(7) Nielsen, C. B.; Angerhofer, A.; Abboud, K. A.; Reynolds, J. R. Discrete Photopatternable π-Conjugated Oligomers for Electrochromic Devices. *J. Am. Chem. Soc.* **2008**, *130*, 9734–9746

(8) Beaujuge, P. M.; Reynolds, J. R. Color Control in π-Conjugated Organic Polymers for Use in Electrochromic Devices. *Chem. Rev.* **2010**, *110*, 268–320

(9) Berggren, M.; Richter-Dahlfors, A. Organic Bioelectronics. *Adv. Mater.* **2007**, *19*, 3201–3213

(10) Rivnay, J.; Owens, R. M.; Malliaras, G. G. The Rise of Organic Bioelectronics. *Chem. Mater.* **2014**, *26*, 679–685

(11) Someya, T.; Bao, Z.; Malliaras, G. G. The Rise of Plastic Bioelectronics. *Nature* **2016**, *540*, 379–385

(12) Simon, D. T.; Kurup, S.; Larsson, K. C.; Hori, R.; Tybrandt, K.; Goiny, M.; Jager, E. W. H.; Berggren, M.; Canlon, B.; Richter-Dahlfors, A. Organic Electronics for Precise Delivery of Neurotransmitters to Modulate Mammalian Sensory Function. *Nat. Mater.* **2009**, *8*, 742–746

(13) Khodagholy, D.; Doublet, T.; Quilichini, P.; Gurfinkel, M.; Leleux, P.; Ghestem, A.; Ismailova, E.; Hervé, T.; Sanaur, S.; Bernard, C.; Malliaras, G. G. In Vivo Recordings of Brain Activity Using Organic Transistors. *Nat. Commun.* **2013**, *4*, 1575

(14) Burgt, Y. van de; Lubberman, E.; Fuller, E. J.; Keene, S. T.; Faria, G. C.; Agarwal, S.; Marinella, M. J.; Talin, A. A.; Salleo, A. A non-volatile organic electrochemical device as a low-voltage artificial synapse for neuromorphic computing. *Nat. Mater.* **2017**, *16*, 414–418

(15) Ohayon, D.; Nikiforidis, G.; Savva, A.; Giugni, A.; Wustoni, S.; Palanisamy, T.; Chen, X.; Maria, I. P.; Di Fabrizio, E.; Costa, P. M. F. J.; McCulloch, I.; Inal, S. Biofuel powered glucose detection in bodily fluids with an n-type conjugated polymer. *Nat. Mater.* **2020**, *19*, 456–463

(16) White, H. S.; Kittlesen, G. P.; Wrighton, M. S. Chemical Derivatization of an Array of Three Gold Microelectrodes with Polypyrrole: Fabrication of a Molecule-Based Transistor. *J. Am. Chem. Soc.* **1984**, *106*, 5375–5377

(17) Strakosas, X.; Bongo, M.; Owens, R. M. The Organic Electrochemical Transistor for Biological Applications. *J. Appl. Polym. Sci.* **2015**, *132*, 41735

(18) Rivnay, J.; Inal, S.; Salleo, A.; Owens, R. M.; Berggren, M.; Malliaras, G. G. Organic Electrochemical Transistors. *Nat. Rev. Mater.* **2018**, *3*, 17086

(19) Borges-González, J.; Kousseff, C. J.; Nielsen, C. B. Organic Semiconductors for Biological Sensing. *J. Mater. Chem. C* **2019**, *7*, 1111–1130

(20) Kim, S.-M.; Kim, C.-H.; Kim, Y.; Kim, N.; Lee, W.-J.; Lee, E.-H.; Kim, D.; Park, S.; Lee, K.; Rivnay, J.; Yoon, M.-H. Influence of PEDOT:PSS Crystallinity and Composition on Electrochemical Transistor Performance and Long-Term Stability. *Nat. Commun.* **2018**, *9*,

3858

(21) Travaglini, L.; Micolich, A. P.; Cazorla, C.; Zeglio, E.; Lauto, A.; Mawad, D. Single-Material OECT-Based Flexible Complementary Circuits Featuring Polyaniline in Both Conducting Channels. *Adv. Funct. Mater.* **2021**, *31*, 2007205

(22) Kim, Y.; Noh, H.; Paulsen, B. D.; Kim, J.; Jo, I. Y.; Ahn, H. J.; Rivnay, J.; Yoon, M. H. Strain-Engineering Induced Anisotropic Crystallite Orientation and Maximized Carrier Mobility for High-Performance Microfiber-Based Organic Bioelectronic Devices. *Adv. Mater.* **2021**, *33*, 2007550

(23) Nielsen, C. B.; Giovannitti, A.; Sbircea, D.-T. T.; Bandiello, E.; Niazi, M. R.; Hanifi, D. A.; Sessolo, M.; Amassian, A.; Malliaras, G. G.; Rivnay, J.; McCulloch, I. Molecular Design of Semiconducting Polymers for High- Performance Organic Electrochemical Transistors. *J. Am. Chem. Soc.* **2016**, *138*, 10252–10259

(24) Giovannitti, A.; Nielsen, C. B.; Sbircea, D.-T. T.; Inal, S.; Donahue, M.; Niazi, M. R.; Hanifi, D. A.; Amassian, A.; Malliaras, G. G.; Rivnay, J.; McCulloch, I. N-Type Organic Electrochemical Transistors with Stability in Water. *Nat. Commun.* **2016**, *7*, 13066

(25) Savagian, L. R.; Österholm, A. M.; Ponder, J. F.; Barth, K. J.; Rivnay, J.; Reynolds, J. R. Balancing Charge Storage and Mobility in an Oligo(Ether) Functionalized Dioxythiophene Copolymer for Organic- and Aqueous- Based Electrochemical Devices and Transistors. *Adv. Mater.* **2018**, *30*, 1804647

(26) Parr, Z. S.; Halaksa, R.; Finn, P. A.; Rashid, R. B.; Kovalenko, A.; Weiter, M.; Rivnay, J.; Krajčovič, J.; Nielsen, C. B. Glycolated Thiophene-Tetrafluorophenylene Copolymers for Bioelectronic Applications: Synthesis by Direct Heteroarylation Polymerisation. *ChemPlusChem* **2019**, *84*, 1384–1390

(27) Giovannitti, A.; Sbircea, D.-T.; Inal, S.; Nielsen, C. B.; Bandiello, E.; Hanifi, D. A.; Sessolo, M.; Malliaras, G. G.; McCulloch, I.; Rivnay, J. Controlling the Mode of Operation of Organic

Transistors through Side-Chain Engineering. *Proc. Natl. Acad. Sci.* **2016**, *113*, 12017–12022

(28) Moser, M.; Hidalgo, T. C.; Surgailis, J.; Gladisch, J.; Ghosh, S.; Sheelamanthula, R.; Thiburce, Q.; Giovannitti, A.; Salleo, A.; Gasparini, N.; Wadsworth, A.; Zozoulenko, I.; Berggren, M.; Stavrinidou, E.; Inal, S.; McCulloch, I. Side Chain Redistribution as a Strategy to Boost Organic Electrochemical Transistor Performance and Stability. *Adv. Mater.* **2020**, *32*, 2002748

(29) Inal, S.; Rivnay, J.; Suiu, A.-O.; Malliaras, G. G.; McCulloch, I. Conjugated Polymers in Bioelectronics. *Acc. Chem. Res.* **2018**, *51*, 1368–1376

(30) Paulsen, B. D.; Tybrandt, K.; Stavrinidou, E.; Rivnay, J. Organic Mixed Ionic–Electronic Conductors. *Nat. Mater.* **2020**, *19*, 13–26

(31) Facchetti, A. Semiconductors for Organic Transistors. *Mater. Today* **2007**, *10*, 28–37

(32) Gsänger, M.; Bialas, D.; Huang, L.; Stolte, M.; Würthner, F. Organic Semiconductors Based on Dyes and Color Pigments. *Adv. Mater.* **2016**, *28*, 3615–3645

(33) Paterson, A. F.; Singh, S.; Fallon, K. J.; Hodsden, T.; Han, Y.; Schroeder, B. C.; Bronstein, H.; Heeney, M.; McCulloch, I.; Anthopoulos, T. D. Recent Progress in High-Mobility Organic Transistors: A Reality Check. *Adv. Mater.* **2018**, *30*, 1801079

(34) Brédas, J. L.; Calbert, J. P.; Da Silva Filho, D. A.; Cornil, J. Organic Semiconductors: A Theoretical Characterization of the Basic Parameters Governing Charge Transport. *Proc. Natl. Acad. Sci. U. S. A.* **2002**, *99*, 5804–5809

(35) Illig, S.; Eggeman, A. S.; Troisi, A.; Jiang, L.; Warwick, C.; Nikolka, M.; Schweicher, G.; Yeates, S. G.; Geerts, Y. H.; Anthony, J. E.; Sirringhaus, H. Reducing Dynamic Disorder in Small-Molecule Organic Semiconductors by Suppressing Large-Amplitude Thermal Motions. *Nat. Commun.* **2016**, *7*, 10736

(36) Liu, C.; Minari, T.; Lu, X.; Kumatani, A.; Takimiya, K.; Tsukagoshi, K. Solution-Processable Organic Single Crystals with Bandlike Transport in Field-Effect Transistors. *Adv. Mater.* **2011**, *23*, 523–526

(37) Takimiya, K.; Bulgarevich, K.; Abbas, M.; Horiuchi, S.; Ogaki, T.; Kawabata, K.; Ablat, A. "Manipulation" of Crystal Structure by Methylthiolation Enabling Ultrahigh Mobility in a Pyrene-Based Molecular Semiconductor. *Adv. Mater.* **2021**, 2102914

(38) Podzorov, V.; Menard, E.; Borissov, A.; Kiryukhin, V.; Rogers, J. A.; Gershenson, M. E. Intrinsic Charge Transport on the Surface of Organic Semiconductors. *Phys. Rev. Lett.* **2004**, *93*, 086602

(39) Mei, Y.; Diemer, P. J.; Niazi, M. R.; Hallani, R. K.; Jarolimek, K.; Day, C. S.; Risko, C.; Anthony, J. E.; Amassian, A.; Jurchescu, O. D. Crossover from Band-like to Thermally Activated Charge Transport in Organic Transistors Due to Strain-Induced Traps. *Proc. Natl. Acad. Sci. U. S. A.* **2017**, *114*, E6739–E6748

(40) Fratini, S.; Nikolka, M.; Salleo, A.; Schweicher, G.; Sirringhaus, H. Charge Transport in High-Mobility Conjugated Polymers and Molecular Semiconductors. *Nat. Mater.* **2020**, *19*, 491–502

(41) Rivnay, J.; Jimison, L. H.; Northrup, J. E.; Toney, M. F.; Noriega, R.; Lu, S.; Marks, T. J.; Facchetti, A.; Salleo, A. Large Modulation of Carrier Transport by Grain-Boundary Molecular Packing and Microstructure in Organic Thin Films. *Nat. Mater.* **2009**, *8*, 952–958

(42) Wegner, B.; Lungwitz, D.; Mansour, A. E.; Tait, C. E.; Tanaka, N.; Zhai, T.; Duhm, S.; Forster, M.; Behrends, J.; Shoji, Y.; Opitz, A.; Scherf, U.; List-Kratochvil, E. J. W.; Fukushima, T.; Koch, N. An Organic Borate Salt with Superior P-Doping Capability for Organic Semiconductors. *Adv. Sci.* **2020**, *7*, 2001322

(43) H. H. Choi, K. Cho, C. D. F. et al.; Choi, H. H.; Cho, K.; Frisbie, C. D.; Sirringhaus, H.; Podzorov, V. Critical Assessment of Charge Carrier Mobility Extraction. *Nat. Mater.* **2018**, *17*, 2–7

(44) McCulloch, I.; Salleo, A.; Chabinyc, M. Avoid the Kinks When Measuring Mobility. *Science* **2016**, *352*, 1521–1522

(45) Liu, C.; Li, G.; Di Pietro, R.; Huang, J.; Noh, Y. Y.; Liu, X.; Minari, T. Device Physics of

Contact Issues for the Overestimation and Underestimation of Carrier Mobility in Field-Effect Transistors. *Phys. Rev. Appl.* **2017**, *8*, 034020

(46) Takeya, J.; Yamagishi, M.; Tominari, Y.; Hirahara, R.; Nakazawa, Y.; Nishikawa, T.; Kawase, T.; Shimoda, T.; Ogawa, S. Very High-Mobility Organic Single-Crystal Transistors with in-Crystal Conduction Channels. *Appl. Phys. Lett.* **2007**, *90*, 102120

(47) Reyes-Martinez, M. A.; Crosby, A. J.; Briseno, A. L. Rubrene Crystal Field-Effect Mobility Modulation via Conducting Channel Wrinkling. *Nat. Commun.* **2015**, *6*, 6948

(48) Anthony, J. E.; Brooks, J. S.; Eaton, D. L.; Parkin, S. R. Functionalized Pentacene: Improved Electronic Properties from Control of Solid-State Order. *J. Am. Chem. Soc.* **2001**, *123*, 9482–9483

(49) Lamport, Z. A.; Barth, K. J.; Lee, H.; Gann, E.; Engmann, S.; Chen, H.; Guthold, M.; McCulloch, I.; Anthony, J. E.; Richter, L. J.; DeLongchamp, D. M.; Jurchescu, O. D. A Simple and Robust Approach to Reducing Contact Resistance in Organic Transistors. *Nat. Commun.* **2018**, *9*, 5130

(50) Zeidell, A. M.; Jennings, L.; Frederickson, C. K.; Ai, Q.; Dressler, J. J.; Zakharov, L. N.; Risko, C.; Haley, M. M.; Jurchescu, O. D. Organic Semiconductors Derived from Dinaphtho-Fused s-Indacenes: How Molecular Structure and Film Morphology Influence Thin-Film Transistor Performance. *Chem. Mater.* **2019**, *31*, 6962–6970

(51) Jurchescu, O. D.; Subramanian, S.; Kline, R. J.; Hudson, S. D.; Anthony, J. E.; Jackson, T. N.; Gundlach, D. J. Organic Single-Crystal Field-Effect Transistors of a Soluble Anthradithiophene. *Chem. Mater.* **2008**, *20*, 6733–6737

(52) Mushrush, M.; Facchetti, A.; Lefenfeld, M.; Katz, H. E.; Marks, T. J. Easily Processable Phenylene-Thiophene-Based Organic Field-Effect Transistors and Solution-Fabricated Nonvolatile Transistor Memory Elements. *J. Am. Chem. Soc.* **2003**, *125*, 9414–9423

(53) Takimiya, K.; Ebata, H.; Sakamoto, K.; Izawa, T.; Otsubo, T.; Kunugi, Y. 2,7-

Diphenyl[1]Benzothieno[3,2-*b*]Benzothiophene, A New Organic Semiconductor for Air-Stable Organic Field-Effect Transistors with Mobilities up to 2.0 $cm^2 V^{-1} s^{-1}$. *J. Am. Chem. Soc.* **2006**, *128*, 12604–12605

(54) Ebata, H.; Izawa, T.; Miyazaki, E.; Takimiya, K.; Ikeda, M.; Kuwabara, H.; Yui, T. Highly Soluble [1]Benzothieno[3,2-*b*]Benzothiophene (BTBT) Derivatives for High-Performance, Solution-Processed Organic Field-Effect Transistors. *J. Am. Chem. Soc.* **2007**, *129*, 15732–15733

(55) Minemawari, H.; Yamada, T.; Matsui, H.; Tsutsumi, J. Y.; Haas, S.; Chiba, R.; Kumai, R.; Hasegawa, T. Inkjet Printing of Single-Crystal Films. *Nature* **2011**, *475*, 364–367

(56) Izawa, T.; Miyazaki, E.; Takimiya, K. Molecular Ordering of High-Performance Soluble Molecular Semiconductors and Re-Evaluation of Their Field-Effect Transistor Characteristics. *Adv. Mater.* **2008**, *20*, 3388–3392

(57) Ma, Z.; Geng, H.; Wang, D.; Shuai, Z. Influences of Alkyl Side-Chain Length on the Carrier Mobility in Organic Semiconductors: Herringbone vs. Pi-Pi Stacking. *J. Mater. Chem. C* **2016**, *4*, 4546–4555

(58) Izawa, T.; Miyazaki, E.; Takimiya, K. Solution-Processible Organic Semiconductors Based on Selenophene-Containing Heteroarenes, 2,7-Dialkyl[1]Benzoselenopheno[3,2-*b*][1]Benzoselenophenes (Cn-BSBSs): Syntheses, Properties, Molecular Arrangements, and Field-Effect Transistor Characteristics. *Chem. Mater.* **2009**, *21*, 903–912

(59) Kang, M. J.; Doi, I.; Mori, H.; Miyazaki, E.; Takimiya, K.; Ikeda, M.; Kuwabara, H. Alkylated Dinaphtho[2,3-*b*:2′,3′-*f*]Thieno[3,2-*b*]Thiophenes (Cn-DNTTs): Organic Semiconductors for High-Performance Thin-Film Transistors. *Adv. Mater.* **2011**, *23*, 1222–1225

(60) Schweicher, G.; D'Avino, G.; Ruggiero, M. T.; Harkin, D. J.; Broch, K.; Venkateshvaran, D.; Liu, G.; Richard, A.; Ruzié, C.; Armstrong, J.; Kennedy, A. R.; Shankland, K.; Takimiya, K.; Geerts, Y. H.; Zeitler, J. A.; Fratini, S.; Sirringhaus, H. Chasing the "Killer" Phonon Mode for

the Rational Design of Low-Disorder, High-Mobility Molecular Semiconductors. *Adv. Mater.* **2019**, *31*, 1902407

(61) Okamoto, T.; Yu, C. P.; Mitsui, C.; Yamagishi, M.; Ishii, H.; Takeya, J. Bent-Shaped p -Type Small-Molecule Organic Semiconductors: A Molecular Design Strategy for Next-Generation Practical Applications. *J. Am. Chem. Soc.* **2020**, *142*, 9083–9096

(62) He, P.; Tu, Z.; Zhao, G.; Zhen, Y.; Geng, H.; Yi, Y.; Wang, Z.; Zhang, H.; Xu, C.; Liu, J.; Lu, X.; Fu, X.; Zhao, Q.; Zhang, X.; Ji, D.; Jiang, L.; Dong, H.; Hu, W. Tuning the Crystal Polymorphs of Alkyl Thienoacene via Solution Self-Assembly toward Air-Stable and High-Performance Organic Field-Effect Transistors. *Adv. Mater.* **2015**, *27*, 825–830

(63) Takimiya, K.; Osaka, I.; Mori, T.; Nakano, M. Organic Semiconductors Based on [1]Benzothieno[3,2-*b*][1] Benzothiophene Substructure. *Acc. Chem. Res.* **2014**, *47*, 1493–1502.

(64) De Leeuw, D. M.; Simenon, M. M. J.; Brown, A. R.; Einerhand, R. E. F. Stability of N-Type Doped Conducting Polymers and Consequences for Polymeric Microelectronic Devices. *Synth. Met.* **1997**, *87*, 53–59

(65) Jones, B. A.; Facchetti, A.; Wasielewski, M. R.; Marks, T. J. Tuning Orbital Energetics in Arylene Diimide Semiconductors. Materials Design for Ambient Stability of n-Type Charge Transport. *J. Am. Chem. Soc.* **2007**, *129*, 15259–15278

(66) Dhar, J.; Salzner, U.; Patil, S. Trends in Molecular Design Strategies for Ambient Stable N-Channel Organic Field Effect Transistors. *J. Mater. Chem. C* **2017**, *5*, 7404–7430

(67) Dennler, G.; Scharber, M. C.; Brabec, C. J. Polymer-Fullerene Bulk-Heterojunction Solar Cells. *Adv. Mater.* **2009**, *21*, 1323–1338

(68) Hummelen, J. C.; Knight, B. W.; Lepeq, F.; Wudl, F.; Yao, J.; Wilkins, C. L. Preparation and Characterization of Fulleroid and Methanofullerene Derivatives. *J. Org. Chem.* **1995**, *60*, 532–538

(69) Meijer, E. J.; De Leeuw, D. M.; Setayesh, S.; Van Veenendaal, E.; Huisman, B. H.; Blom, P. W. M.; Hummelen, J. C.; Scherf, U.; Klapwijk, T. M. Solution-Processed Ambipolar Organic Field-Effect Transistors and Inverters. *Nat. Mater.* **2003**, *2*, 678–682

(70) Scharber, M. C.; Mühlbacher, D.; Koppe, M.; Denk, P.; Waldauf, C.; Heeger, A. J.; Brabec, C. J. Design Rules for Donors in Bulk-Heterojunction Solar Cells - Towards 10 % Energy-Conversion Efficiency. *Adv. Mater.* **2006**, *18*, 789–794

(71) Chikamatsu, M.; Itakura, A.; Yoshida, Y. High-Performance n-Type Organic Thin-Film Transistors Based on Solution-Processable Perfluoroalkyl-Substituted C 60 Derivatives. *Chem. Mater.* **2008**, *20*, 7365–7367.

(72) Yang, X.; Van Duren, J. K. J.; Rispens, M. T.; Hummelen, J. C.; Janssen, R. A. J.; Michels, M. A. J.; Loos, J. Crystalline Organization of a Methanofullerene as Used for Plastic Solar-Cell Applications. *Adv. Mater.* **2004**, *16*, 802–806

(73) Itaka, K.; Yamashiro, M.; Yamaguchi, J.; Haemori, M.; Yaginuma, S.; Matsumoto, Y.; Kondo, M.; Koinuma, H. High-Mobility C60 Field-Effect Transistors Fabricated on Molecular-Wetting Controlled Substrates. *Adv. Mater.* **2006**, *18*, 1713–1716

(74) Anthopoulos, T. D.; Singh, B.; Marjanovic, N.; Sariciftci, N. S.; Montaigne Ramil, A.; Sitter, H.; Cölle, M.; De Leeuw, D. M. High Performance n -Channel Organic Field-Effect Transistors and Ring Oscillators Based on C60 Fullerene Films. *Appl. Phys. Lett.* **2006**, *89*, 213504

(75) Li, H.; Tee, B. C. K.; Cha, J. J.; Cui, Y.; Chung, J. W.; Lee, S. Y.; Bao, Z. High-Mobility Field-Effect Transistors from Large-Area Solution-Grown Aligned C60 Single Crystals. *J. Am. Chem. Soc.* **2012**, *134*, 2760–2765

(76) Li, C. Z.; Chueh, C. C.; Yip, H. L.; Zou, J.; Chen, W. C.; Jen, A. K. Y. Evaluation of Structure-Property Relationships of Solution-Processible Fullerene Acceptors and Their n-Channel Field-Effect Transistor Performance. *J. Mater. Chem.* **2012**, *22*, 14976–14981

(77) Anthopoulos, T. D.; Kooistra, F. B.; Wondergem, H. J.; Kronholm, D.; Hummelen, J. C.; De Leeuw, D. M. Air-Stable n-Channel Organic Transistors Based on a Soluble C84 Fullerene Derivative. *Adv. Mater.* **2006**, *18*, 1679–1684

(78) Yu, H.; Cho, H. H.; Cho, C. H.; Kim, K. H.; Kim, D. Y.; Kim, B. J.; Oh, J. H. Polarity and Air-Stability Transitions in Field-Effect Transistors Based on Fullerenes with Different Solubilizing Groups. *ACS Appl. Mater. Interfaces* **2013**, *5*, 4865–4871

(79) Nielsen, C. B.; Holliday, S.; Chen, H.-Y.; Cryer, S. J.; McCulloch, I. Non-Fullerene Electron Acceptors for Use in Organic Solar Cells. *Acc. Chem. Res.* **2015**, *48*, 2803–2812

(80) Wadsworth, A.; Moser, M.; Marks, A.; Little, M. S.; Gasparini, N.; Brabec, C. J.; Baran, D.; McCulloch, I. Critical Review of the Molecular Design Progress in Non-Fullerene Electron Acceptors towards Commercially Viable Organic Solar Cells. *Chem. Soc. Rev.* **2018**, *48*, 1596–1625

(81) Zhan, X.; Facchetti, A.; Barlow, S.; Marks, T. J.; Ratner, M. A.; Wasielewski, M. R.; Marder, S. R. Rylene and Related Diimides for Organic Electronics. *Adv. Mater.* **2011**, *23*, 268–284

(82) Laquindanum, J. G.; Katz, H. E.; Dodabalapur, A.; Lovinger, A. J. N-Channel Organic Transistor Materials Based on Naphthalene Frameworks. *J. Am. Chem. Soc.* **1996**, *118*, 11331–11332

(83) Welford, A.; Maniam, S.; Gann, E.; Jiao, X.; Thomsen, L.; Langford, S. J.; McNeill, C. R. Influence of Alkyl Side-Chain Type and Length on the Thin Film Microstructure and OFET Performance of Naphthalene Diimide-Based Organic Semiconductors. *Org. Electron.* **2019**, *75*, 105378

(84) Komissarova, E. A.; Dominskiy, D. I.; Zhulanov, V. E.; Abashev, G. G.; Siddiqui, A.; Singh, S. P.; Sosorev, A. Y.; Paraschuk, D. Y. Unraveling the Unusual Effect of Fluorination on Crystal Packing in an Organic Semiconductor. *Phys. Chem. Chem. Phys.* **2020**, *22*, 1665–1673

(85) Stoeckel, M. A.; Olivier, Y.; Gobbi, M.; Dudenko, D.; Lemaur, V.; Zbiri, M.; Guilbert, A. A.

Y.; D'Avino, G.; Liscio, F.; Migliori, A.; Ortolani, L.; Demitri, N.; Jin, X.; Jeong, Y. G.; Liscio, A.; Nardi, M. V.; Pasquali, L.; Razzari, L.; Beljonne, D.; Samorì, P.; Orgiu, E. Analysis of External and Internal Disorder to Understand Band-Like Transport in n-Type Organic Semiconductors. *Adv. Mater.* **2021**, *33*, 2007870

(86) Tilley, A. J.; Pensack, R. D.; Lee, T. S.; Djukic, B.; Scholes, G. D.; Seferos, D. S. Ultrafast Triplet Formation in Thionated Perylene Diimides. *J. Phys. Chem. C* **2014**, *118*, 9996–10004

(87) Gsänger, M.; Oh, J. H.; Könemann, M.; Höffken, H. W.; Krause, A. M.; Bao, Z.; Würthner, F. A Crystal-Engineered Hydrogen-Bonded Octachloroperylene Diimide with a Twisted Core: An n-Channel Organic Semiconductor. *Angew. Chemie - Int. Ed.* **2010**, *49*, 740–743

(88) Ha, Y. H.; Oh, J. G.; Park, S.; Kwon, S. K.; An, T. K.; Jang, J.; Kim, Y. H. Novel Naphthalene-Diimide-Based Small Molecule with a Bithiophene Linker for Use in Organic Field-Effect Transistors. *Org. Electron.* **2018**, *63*, 250–256

(89) Luo, H.; He, D.; Zhang, Y.; Wang, S.; Gao, H.; Yan, J.; Cao, Y.; Cai, Z.; Tan, L.; Wu, S.; Wang, L.; Liu, Z. Synthesis of Heterocyclic Core-Expanded Bis-Naphthalene Tetracarboxylic Diimides. *Org. Lett.* **2019**, *21*, 9734–9737

(90) Zhao, Y.; Di, C. A.; Gao, X.; Hu, Y.; Guo, Y.; Zhang, L.; Liu, Y.; Wang, J.; Hu, W.; Zhu, D. All-Solution-Processed, High-Performance n-Channel Organic Transistors and Circuits: Toward Low-Cost Ambient Electronics. *Adv. Mater.* **2011**, *23*, 2448–2453

(91) Zhang, F.; Hu, Y.; Schuettfort, T.; Di, C. A.; Gao, X.; McNeill, C. R.; Thomsen, L.; Mannsfeld, S. C. B.; Yuan, W.; Sirringhaus, H.; Zhu, D. Critical Role of Alkyl Chain Branching of Organic Semiconductors in Enabling Solution-Processed N-Channel Organic Thin-Film Transistors with Mobility of up to 3.50 $cm^2 V^{-1} s^{-1}$. *J. Am. Chem. Soc.* **2013**, *135*, 2338–2349

(92) Lei, T.; Dou, J.; Cao, X.; Wang, J.; Pei, J. Electron-Deficient Poly(P-phenylene Vinylene) Provides Electron Mobility over 1 cm2 $V^{-1} s^{-1}$ under Ambient Conditions. *J. Am. Chem. Soc.*

2013, *135*, 12168–12171

(93) Dou, J. H.; Zheng, Y. Q.; Yao, Z. F.; Lei, T.; Shen, X.; Luo, X. Y.; Yu, Z. A.; Zhang, S. D.; Han, G.; Wang, Z.; Yi, Y.; Wang, J. Y.; Pei, J. A Cofacially Stacked Electron-Deficient Small Molecule with a High Electron Mobility of over 10 cm^2 V^{-1} s^{-1} in Air. *Adv. Mater.* **2015**, *27*, 8051–8055

(94) Dou, J. H.; Zheng, Y. Q.; Yao, Z. F.; Yu, Z. A.; Lei, T.; Shen, X.; Luo, X. Y.; Sun, J.; Zhang, S. D.; Ding, Y. F.; Han, G.; Yi, Y.; Wang, J. Y.; Pei, J.; Dou, J. H.; Zheng, Y. Q.; Yao, Z. F.; Yu, Z. A.; Lei, T.; Shen, X. Fine-Tuning of Crystal Packing and Charge Transport Properties of BDOPV Derivatives through Fluorine Substitution. *J. Am. Chem. Soc.* **2015**, *137*, 15947–15956

(95) Casado, J.; Ortiz, R. P.; Navarrete, J. T. L. Quinoidal Oligothiophenes: New Properties behind an Unconventional Electronic Structure. *Chem. Soc. Rev.* **2012**, *41*, 5672–5686

(96) Pappenfus, T. M.; Chesterfield, R. J.; Frisbie, C. D.; Mann, K. R.; Casado, J.; Raff, J. D.; Miller, L. L. A π-Stacking Terthiophene-Based Quinodimethane Is an n-Channel Conductor in a Thin Film Transistor. *J. Am. Chem. Soc.* **2002**, *124*, 4184–4185

(97) Joseph, V.; Yu, C. H.; Lin, C. C.; Lien, W. C.; Tsai, H. C.; Chen, C. S.; Torimtubun, A. A. A.; Velusamy, A.; Huang, P. Y.; Lee, G. H.; Yau, S. L.; Tung, S. H.; Minari, T.; Liu, C. L.; Chen, M. C. Quinoidal Thioalkyl-Substituted Bithiophene Small Molecule Semiconductors for n-Type Organic Field Effect Transistors. *J. Mater. Chem. C* **2020**, *8*, 15450–15458

(98) Vegiraju, S.; Amelenan Torimtubun, A. A.; Lin, P. S.; Tsai, H. C.; Lien, W. C.; Chen, C. S.; He, G. Y.; Lin, C. Y.; Zheng, D.; Huang, Y. F.; Wu, Y. C.; Yau, S. L.; Lee, G. H.; Tung, S. H.; Wang, C. L.; Liu, C. L.; Chen, M. C.; Facchetti, A. Solution-Processable Quinoidal Dithioalkylterthiophene-Based Small Molecules Pseudo-Pentathienoacenes via an Intramolecular S···S Lock for High-Performance n-Type Organic Field-Effect Transistors. *ACS Appl. Mater. Interfaces* **2020**, *12*, 25081–25091

(99) Zhang, C.; Zang, Y.; Gann, E.; McNeill, C. R.; Zhu, X.; Di, C. A.; Zhu, D. Two-Dimensional π-Expanded Quinoidal Terthiophenes Terminated with Dicyanomethylenes as n-Type Semiconductors for High-Performance Organic Thin-Film Transistors. *J. Am. Chem. Soc.* **2014**, *136*, 16176–16184

(100) Zhang, C.; Zang, Y.; Zhang, F.; Diao, Y.; McNeill, C. R.; Di, C.; Zhu, X.; Zhu, D. Pursuing High-Mobility n-Type Organic Semiconductors by Combination of "Molecule-Framework" and "Side-Chain" Engineering. *Adv. Mater.* **2016**, *28*, 8456–8462

(101) Davies, D. W.; Park, S. K.; Kafle, P.; Chung, H.; Yuan, D.; Strzalka, J. W.; Mannsfeld, S. C. B.; Wang, S. G.; Chen, Y.-S.; Gray, D. L.; Zhu, X.; Diao, Y. Radically Tunable N-Type Organic Semiconductor via Polymorph Control. *Chem. Mater.* **2021**, *33*, 2466–2477

(102) Velusamy, A.; Yu, C. H.; Afraj, S. N.; Lin, C. C.; Lo, W. Y.; Yeh, C. J.; Wu, Y. W.; Hsieh, H. C.; Chen, J.; Lee, G. H.; Tung, S. H.; Liu, C. L.; Chen, M. C.; Facchetti, A. Thienoisoindigo (TII)-Based Quinoidal Small Molecules for High-Performance n-Type Organic Field Effect Transistors. *Adv. Sci.* **2020**, *8*, 2002930

(103) Wang, C.; Qin, Y.; Sun, Y.; Guan, Y. S.; Xu, W.; Zhu, D. Thiophene-Diketopyrrolopyrrole-Based Quinoidal Small Molecules as Solution-Processable and Air-Stable Organic Semiconductors: Tuning of the Length and Branching Position of the Alkyl Side Chain toward a High-Performance n-Channel Organic Field-Effect Tran. *ACS Appl. Mater. Interfaces* **2015**, *7*, 15978–15987

(104) Zhou, Q.; Jiang, Y.; Du, T.; Wang, Z.; Liang, Z.; Han, Y.; Deng, Y.; Tian, H.; Geng, Y. Diketopyrrolopyrrole-Based Small Molecules for Solution-Processed n-Channel Organic Thin Film Transistors. *J. Mater. Chem. C* **2019**, *7*, 13939–13946

(105) Chen, J.; Das, S.; Shao, M.; Li, G.; Lian, H.; Qin, J.; Browning, J. F.; Keum, J. K.; Uhrig, D.; Gu, G.; Xiao, K. Phase Segregation Mechanisms of Small Molecule-polymer Blends Unraveled by Varying Polymer Chain Architecture. *SmartMat.* doi.org/10.1002/smm2.1036

(106) Chou, L. H.; Na, Y.; Park, C. H.; Park, M. S.; Osaka, I.; Kim, F. S.; Liu, C. L. Semiconducting Small Molecule/Polymer Blends for Organic Transistors. *Polymer* **2020**, *191*, 122208

(107) Stingelin, N. On the Phase Behaviour of Organic Semiconductors. *Polym. Int.* **2012**, *61*, 866–873

(108) Balsara, N. P.; Lin, C.; Hammouda, B. Early Stages of Nucleation and Growth in a Polymer Blend. *Phys. Rev. Lett.* **1996**, *77*, 3847–3850

(109) Smith, J.; Hamilton, R.; McCulloch, I.; Stingelin-Stutzmann, N.; Heeney, M.; Bradley, D. D. C.; Anthopoulos, T. D. Solution-Processed Organic Transistors Based on Semiconducting Blends. *J. Mater. Chem.* **2010**, *20*, 2562–2574

(110) Kang, J.; Shin, N.; Do, Y. J.; Prabhu, V. M.; Yoon, D. Y. Structure and Properties of Small Molecule-Polymer Blend Semiconductors for Organic Thin Film Transistors. *J. Am. Chem. Soc.* **2008**, *130*, 12273–12275

(111) Kaimakamis, T.; Pitsalidis, C.; Papamichail, A.; Laskarakis, A.; Logothetidis, S. Organic Transistors Based on Airbrushed Small Molecule-Insulating Polymer Blends with Mobilities Exceeding 1 $cm^2 V^{-1} s^{-1}$. *RSC Adv.* **2016**, *6*, 97077–97083

(112) Madec, M. B.; Smith, P. J.; Malandraki, A.; Wang, N.; Korvink, J. G.; Yeates, S. G. Enhanced Reproducibility of Inkjet Printed Organic Thin Film Transistors Based on Solution Processable Polymer-Small Molecule Blends. *J. Mater. Chem.* **2010**, *20*, 9155–9160

(113) Hoon Park, J.; Lim, H.; Cheong, H.; Min Lee, K.; Chul Sohn, H.; Lee, G.; Im, S. Anisotropic Mobility of Small Molecule-Polymer Blend Channel in Organic Transistor: Characterization of Channel Materials and Orientation. *Org. Electron.* **2012**, *13*, 1250–1254

(114) Onojima, N.; Obata, S.; Nakamura, A.; Hara, K. Influence of Phase-Separated Morphology on Small Molecule/Polymer Blend Organic Field-Effect Transistors Fabricated Using Electrostatic Spray Deposition. *Thin Solid Films* **2017**, *640*, 99–103

(115) Obata, S.; Miyazawa, Y.; Yamanaka, J.; Onojima, N. Environmentally-Friendly Fabrication of

Organic Field-Effect Transistors Based on Small Molecule/Polymer Blend Prepared by Electrostatic Spray Deposition. *Jpn. J. Appl. Phys.* **2019**, *58*, SBBG02

(116) Hamilton, R.; Smith, J.; Ogier, S.; Heeney, M.; Anthony, J. E.; McCulloch, I.; Veres, J.; Bradley, D. D. C.; Anthopoulos, T. D. High-Performance Polymer-Small Molecule Blend Organic Transistors. *Adv. Mater.* **2009**, *21*, 1166–1171

(117) Niazi, M. R.; Li, R.; Abdelsamie, M.; Zhao, K.; Anjum, D. H.; Payne, M. M.; Anthony, J.; Smilgies, D. M.; Amassian, A. Contact-Induced Nucleation in High-Performance Bottom-Contact Organic Thin Film Transistors Manufactured by Large-Area Compatible Solution Processing. *Adv. Funct. Mater.* **2016**, *26*, 2371–2378

(118) Lada, M.; Starink, M. J.; Carrasco, M.; Chen, L.; Miskiewicz, P.; Brookes, P.; Obarowska, M.; Smith, D. C. Morphology Control via Dual Solvent Crystallization for High-Mobility Functionalized Pentacene-Blend Thin Film Transistors. *J. Mater. Chem.* **2011**, *21*, 11232–11238

(119) Teixeira da Rocha, C.; Haase, K.; Zheng, Y.; Löffler, M.; Hambsch, M.; Mannsfeld, S. C. B. Solution Coating of Small Molecule/Polymer Blends Enabling Ultralow Voltage and High-Mobility Organic Transistors. *Adv. Electron. Mater.* **2018**, *4*, 1800141

(120) Bharti, D.; Raghuwanshi, V.; Varun, I.; Mahato, A. K.; Tiwari, S. P. High Performance and Electro-Mechanical Stability in Small Molecule: Polymer Blend Flexible Organic Field-Effect Transistors. *IEEE Electron Device Lett.* **2016**, *37*, 1215–1218

(121) Kim, S. H.; Choi, M. H.; Kim, B. S.; Jang, J.. P-120: High-performance of Ink-jet Printed Organic Thin-film Transistors on Flexible Substrate Using a Small Molecule-polymer Blend. SID Symposium Digest of Technical Papers **2011**, *42*, 1555–1558

(122) Shin, N.; Kang, J.; Richter, L. J.; Prabhu, V. M.; Kline, R. J.; Fischer, D. A.; DeLongchamp, D. M.; Toney, M. F.; Satija, S. K.; Gundlach, D. J.; Purushothaman, B.; Anthony, J. E.; Yoon, D. Y. Vertically Segregated Structure and Properties of Small Molecule-Polymer Blend

Semiconductors for Organic Thin-Film Transistors. *Adv. Funct. Mater.* **2013**, *23*, 366–376

(123) Chung, Y. S.; Shin, N.; Kang, J.; Jo, Y.; Prabhu, V. M.; Satija, S. K.; Kline, R. J.; DeLongchamp, D. M.; Toney, M. F.; Loth, M. A.; Purushothaman, B.; Anthony, J. E.; Yoon, D. Y. Zone-Refinement Effect in Small Molecule-Polymer Blend Semiconductors for Organic Thin-Film Transistors. *J. Am. Chem. Soc.* **2011**, *133*, 412–415

(124) Niazi, M. R.; Li, R.; Qiang Li, E.; Kirmani, A. R.; Abdelsamie, M.; Wang, Q.; Pan, W.; Payne, M. M.; Anthony, J. E.; Smilgies, D. M.; Thoroddsen, S. T.; Giannelis, E. P.; Amassian, A. Solution-Printed Organic Semiconductor Blends Exhibiting Transport Properties on Par with Single Crystals. *Nat. Commun.* **2015**, *6*, 8598

(125) Smith, J.; Zhang, W.; Sougrat, R.; Zhao, K.; Li, R.; Cha, D.; Amassian, A.; Heeney, M.; McCulloch, I.; Anthopoulos, T. D. Solution-Processed Small Molecule-Polymer Blend Organic Thin-Film Transistors with Hole Mobility Greater than 5 cm^2/Vs. *Adv. Mater.* **2012**, *24*, 2441–2446

(126) Zhao, K.; Wodo, O.; Ren, D.; Khan, H. U.; Niazi, M. R.; Hu, H.; Abdelsamie, M.; Li, R.; Li, E. Q.; Yu, L.; Yan, B.; Payne, M. M.; Smith, J.; Anthony, J. E.; Anthopoulos, T. D.; Thoroddsen, S. T.; Ganapathysubramanian, B.; Amassian, A. Vertical Phase Separation in Small Molecule:Polymer Blend Organic Thin Film Transistors Can Be Dynamically Controlled. *Adv. Funct. Mater.* **2016**, *26*, 1737–1746

(127) Smith, J.; Hamilton, R.; Qi, Y.; Kahn, A.; Bradley, D. D. C.; Heeney, M.; McCulloch, I.; Anthopoulos, T. D. The Influence of Film Morphology in High-Mobility Small-Molecule: Polymer Blend Organic Transistors. *Adv. Funct. Mater.* **2010**, *20*, 2330–2337

(128) Panidi, J.; Paterson, A. F.; Khim, D.; Fei, Z.; Han, Y.; Tsetseris, L.; Vourlias, G.; Patsalas, P. A.; Heeney, M.; Anthopoulos, T. D. Remarkable Enhancement of the Hole Mobility in Several Organic Small-Molecules, Polymers, and Small-Molecule:Polymer Blend Transistors by Simple Admixing of the Lewis Acid p-Dopant $B(C_6F_5)_3$. *Adv. Sci.* **2018**, *5*, 1700290

(129) Huang, J.; Du, J.; Cevher, Z.; Ren, Y.; Wu, X.; Chu, Y. Printable and Flexible Phototransistors Based on Blend of Organic Semiconductor and Biopolymer. *Adv. Funct. Mater.* **2017**, *27*, 1604163

(130) Paterson, A. F.; Lin, Y.-H. H.; Mottram, A. D.; Fei, Z.; Niazi, M. R.; Kirmani, A. R.; Amassian, A.; Solomeshch, O.; Tessler, N.; Heeney, M.; Anthopoulos, T. D. The Impact of Molecular P-Doping on Charge Transport in High-Mobility Small-Molecule/Polymer Blend Organic Transistors. *Adv. Electron. Mater.* **2017**, *4*, 1700464

(131) Paterson, A. F.; Treat, N. D.; Zhang, W.; Fei, Z.; Wyatt-Moon, G.; Faber, H.; Vourlias, G.; Patsalas, P. A.; Solomeshch, O.; Tessler, N.; Heeney, M.; Anthopoulos, T. D. Small Molecule/Polymer Blend Organic Transistors with Hole Mobility Exceeding 13 $cm^2 V^{-1} s^{-1}$. *Adv. Mater.* **2016**, *28*, 7791–7798

(132) Basu, A.; Niazi, M. R.; Scaccabarozzi, A. D.; Faber, H.; Fei, Z.; Anjum, D. H.; Paterson, A. F.; Boltalina, O.; Heeney, M.; Anthopoulos, T. D. Impact of P-Type Doping on Charge Transport in Blade-Coated Small-Molecule:Polymer Blend Transistors. *J. Mater. Chem. C* **2020**, *8*, 15368–15376

(133) Paterson, A. F.; Tsetseris, L.; Li, R.; Basu, A.; Faber, H.; Emwas, A. H.; Panidi, J.; Fei, Z.; Niazi, M. R.; Anjum, D. H.; Heeney, M.; Anthopoulos, T. D. Addition of the Lewis Acid $Zn(C_6F_5)_2$ Enables Organic Transistors with a Maximum Hole Mobility in Excess of 20 $cm^2 V^{-1} S^{-1}$. *Adv. Mater.* **2019**, *31*, 1900871

(134) Haase, K.; Teixeira da Rocha, C.; Hauenstein, C.; Zheng, Y.; Hambsch, M.; Mannsfeld, S. C. B. High-Mobility, Solution-Processed Organic Field-Effect Transistors from C8-BTBT:Polystyrene Blends. *Adv. Electron. Mater.* **2018**, *4* , 1800076

(135) Pérez-Rodríguez, A.; Temiño, I.; Ocal, C.; Mas-Torrent, M.; Barrena, E. Decoding the Vertical Phase Separation and Its Impact on C8-BTBT/PS Transistor Properties. *ACS Appl. Mater. Interfaces* **2018**, *10*, 7296–7303

(136) Yuan, Y.; Giri, G.; Ayzner, A. L.; Zoombelt, A. P.; Mannsfeld, S. C. B.; Chen, J.; Nordlund, D.; Toney, M. F.; Huang, J.; Bao, Z. Ultra-High Mobility Transparent Organic Thin Film Transistors Grown by an off-Centre Spin-Coating Method. *Nat. Commun.* **2014**, *5*, 3005

(137) Salzillo, T.; Campos, A.; Babuji, A.; Santiago, R.; Bromley, S. T.; Ocal, C.; Barrena, E.; Jouclas, R.; Ruzie, C.; Schweicher, G.; Geerts, Y. H.; Mas-Torrent, M. Enhancing Long-Term Device Stability Using Thin Film Blends of Small Molecule Semiconductors and Insulating Polymers to Trap Surface-Induced Polymorphs. *Adv. Funct. Mater.* **2020**, *30*, 2006115

(138) Shiwaku, R.; Takeda, Y.; Fukuda, T.; Fukuda, K.; Matsui, H.; Kumaki, D.; Tokito, S. Printed 2 V-Operating Organic Inverter Arrays Employing a Small-Molecule/Polymer Blend. *Sci. Rep.* **2016**, *6*, 34723

(139) Lin, C. C.; Afraj, S. N.; Velusamy, A.; Yu, P. C.; Cho, C. H.; Chen, J.; Li, Y. H.; Lee, G. H.; Tung, S. H.; Liu, C. L.; Chen, M. C.; Facchetti, A. A Solution Processable Dithioalkyl Dithienothiophene (DSDTT) Based Small Molecule and Its Blends for High Performance Organic Field Effect Transistors. *ACS Nano* **2021**, *15*, 727–738

(140) Orgiu, E.; Masillamani, A. M.; Vogel, J.-O.; Treossi, E.; Kiersnowski, A.; Kastler, M.; Pisula, W.; Dötz, F.; Palermo, V.; Samorì, P. Enhanced Mobility in P3HT-Based OTFTs upon Blending with a Phenylene–Thiophene–Thiophene–Phenylene Small Molecule. *Chem. Commun.* **2012**, *48*, 1562–1564

(141) Kang, M.; Hwang, H.; Park, W. T.; Khim, D.; Yeo, J. S.; Kim, Y.; Kim, Y. J.; Noh, Y. Y.; Kim, D. Y. Ambipolar Small-Molecule:Polymer Blend Semiconductors for Solution-Processable Organic Field-Effect Transistors. *ACS Appl. Mater. Interfaces* **2017**, *9*, 2686–2692

(142) Zhong, H.; Smith, J.; Rossbauer, S.; White, A. J. P.; Anthopoulos, T. D.; Heeney, M. Air-Stable and High-Mobility n-Channel Organic Transistors Based on Small-Molecule/Polymer Semiconducting Blends. *Adv. Mater.* **2012**, *24*, 3205–3211

(143) Campos, A.; Riera-Galindo, S.; Puigdollers, J.; Mas-Torrent, M. Reduction of Charge Traps

and Stability Enhancement in Solution-Processed Organic Field-Effect Transistors Based on a Blended n-Type Semiconductor. *ACS Appl. Mater. Interfaces* **2018**, *10*, 15952–15961

(144) Amegadze, P. S. K.; Noh, Y. Y. Development of High-Performance n-Type Organic Thin-Film Transistors Using a Small-Molecule Polymer Blend. *Thin Solid Films* **2014**, *556*, 414–418

(145) Nicolai, H. T.; Kuik, M.; Wetzelaer, G. A. H.; De Boer, B.; Campbell, C.; Risko, C.; Brédas, J. L.; Blom, P. W. M. Unification of Trap-Limited Electron Transport in Semiconducting Polymers. *Nat. Mater.* **2012**, *11*, 882–887

(146) Giovannitti, A.; Thorley, K. J.; Nielsen, C. B.; Li, J.; Donahue, M. J.; Malliaras, G. G.; Rivnay, J.; McCulloch, I. Redox-Stability of Alkoxy-BDT Copolymers and Their Use for Organic Bioelectronic Devices. *Adv. Funct. Mater.* **2018**, *28*, 1706325

(147) Giovannitti, A.; Rashid, R. B.; Thiburce, Q.; Paulsen, B. D.; Cendra, C.; Thorley, K.; Moia, D.; Mefford, J. T.; Hanifi, D.; Weiyuan, D.; Moser, M.; Salleo, A.; Nelson, J.; McCulloch, I.; Rivnay, J. Energetic Control of Redox-Active Polymers toward Safe Organic Bioelectronic Materials. *Adv. Mater.* **2020**, *31*, 1908047

(148) Nikolka, M.; Nasrallah, I.; Rose, B.; Ravva, M. K.; Broch, K.; Sadhanala, A.; Harkin, D.; Charmet, J.; Hurhangee, M.; Brown, A.; Illig, S.; Too, P.; Jongman, J.; McCulloch, I.; Bredas, J.-L.; Sirringhaus, H. High Operational and Environmental Stability of High-Mobility Conjugated Polymer Field-Effect Transistors through the Use of Molecular Additives. *Nat. Mater.* **2017**, *16*, 356–362

(149) Nikolka, M.; Schweicher, G.; Armitage, J.; Nasrallah, I.; Jellett, C.; Guo, Z.; Hurhangee, M.; Sadhanala, A.; McCulloch, I.; Nielsen, C. B.; Sirringhaus, H. Performance Improvements in Conjugated Polymer Devices by Removal of Water-Induced Traps. *Adv. Mater.* **2018**, *30*, 1801874

(150) Sung, A.; Ling, M. M.; Tang, M. L.; Bao, Z.; Locklin, J. Correlating Molecular Structure to

Field-Effect Mobility: The Investigation of Side-Chain Functionality in Phenylene−Thiophene Oligomers and Their Application in Field Effect Transistors *Chem. Mater.* **2007**, *19*, 2342–2351

(151) Vaidyanathan, S.; Do, F.; Katz, H. E.; Lawrentz, U.; Granstrom, J.; Reichmanis, E. Investigation of Solubility-Field Effect Mobility Orthogonality in Substituted Phenylene-Thiophene Co-Oligomers. *Chem. Mater.* **2007**, *19*, 4676–4681

(152) Huang, J.; Miragliotta, J.; Becknell, A.; Katz, H. E. Hydroxy-Terminated Organic Semiconductor-Based Field-Effect Transistors for Phosphonate Vapor Detection. *J. Am. Chem. Soc.* **2007**, *129*, 9366–9376

(153) Pacheco-Moreno, C. M.; Schreck, M.; Scaccabarozzi, A. D.; Bourgun, P.; Wantz, G.; Stevens, M. M.; Dautel, O. J.; Stingelin, N. The Importance of Materials Design to Make Ions Flow: Toward Novel Materials Platforms for Bioelectronics Applications. *Adv. Mater.* **2016**, *29*, 1604446

(154) Nicolini, T.; Surgailis, J.; Savva, A.; Scaccabarozzi, A. D.; Nakar, R.; Thuau, D.; Wantz, G.; Richter, L. J.; Dautel, O.; Hadziioannou, G.; Stingelin, N. A Low-Swelling Polymeric Mixed Conductor Operating in Aqueous Electrolytes. *Adv. Mater.* **2020**, *33*, 2005723

(155) Parr, Z. S.; Rashid, R. B.; Paulsen, B. D.; Poggi, B.; Tan, E.; Freeley, M.; Palma, M.; Abrahams, I.; Rivnay, J.; Nielsen, C. B. Semiconducting Small Molecules as Active Materials for P-Type Accumulation Mode Organic Electrochemical Transistors. *Adv. Electron. Mater.* **2020**, *6*, 2000215

(156) Guilbert, A. A. Y.; Parr, Z. S.; Kreouzis, T.; Woods, D. J.; Sprick, R. S.; Abrahams, I.; Nielsen, C. B.; Zbiri, M. Effect of Substituting Non-Polar Chains with Polar Chains on the Structural Dynamics of Small Organic Molecule and Polymer Semiconductors. *Phys. Chem. Chem. Phys.* **2021**, *23*, 7462–7471

(157) Sherck, N.; Webber, T.; Brown, D. R.; Keller, T.; Barry, M.; Destefano, A.; Jiao, S.;

Segalman, R. A.; Fredrickson, G. H.; Shell, M. S.; Han, S. End-to-End Distance Probability Distributions of Dilute Poly(Ethylene Oxide) in Aqueous Solution. *J. Am. Chem. Soc.* **2020**, *142*, 19631–19641

(158) Alessi, M. L.; Norman, A. I.; Knowlton, S. E.; Ho, D. L.; Greer, S. C. Helical and Coil Conformations of Poly(Ethylene Glycol) in Isobutyric Acid and Water. *Macromolecules* **2005**, *38*, 9333–9340

(159) Roberts, M. E.; Mannsfeld, S. C. B.; Queraltó, N.; Reese, C.; Locklin, J.; Knoll, W.; Bao, Z. Water-Stable Organic Transistors and Their Application in Chemical and Biological Sensors. *Proc. Natl. Acad. Sci.* **2008**, *105*, 12134–12139

(160) Bettinger, C. J.; Bao, Z. Organic Thin-Film Transistors Fabricated on Resorbable Biomaterial Substrates. *Adv. Mater.* **2010**, *22*, 651–655

(161) Torsi, L.; Farinola, G. M.; Marinelli, F.; Tanese, M. C.; Omar, O. H.; Valli, L.; Babudri, F.; Palmisano, F.; Zambonin, P. G.; Naso, F. A Sensitivity-Enhanced Field-Effect Chiral Sensor. *Nat. Mater.* **2008**, *7*, 412–417

(162) Squillaci, M. A.; Ferlauto, L.; Zagranyarski, Y.; Milita, S.; Müllen, K.; Samorì, P. Self-Assembly of an Amphiphilic π-Conjugated Dyad into Fibers: Ultrafast and Ultrasensitive Humidity Sensor. *Adv. Mater.* **2015**, *27*, 3170–3174

(163) Squillaci, M. A.; Cipriani, A.; Melucci, M.; Zambianchi, M.; Caminati, G.; Samorì, P. Self-Assembly of Functionalized Oligothiophene into Hygroscopic Fibers: Fabrication of Highly Sensitive and Fast Humidity Sensors. *Adv. Electron. Mater.* **2018**, *4*, 1700382

(164) Liu, Z.; Nalluri, S. K. M.; Stoddart, J. F. Surveying Macrocyclic Chemistry: From Flexible Crown Ethers to Rigid Cyclophanes. *Chem. Soc. Rev.* **2017**, *46*, 2459–2478

(165) Marsella, M. J.; Swager, T. M. Designing Conducting Polymer-Based Sensors: Selective Ionochromic Response in Crown Ether-Containing Polythiophenes. *J. Am. Chem. Soc.* **1993**, *115*, 12214–12215

(166) Giovannitti, A.; Nielsen, C. B.; Rivnay, J.; Kirkus, M.; Harkin, D. J.; White, A. J. P.; Sirringhaus, H.; Malliaras, G. G.; McCulloch, I. Sodium and Potassium Ion Selective Conjugated Polymers for Optical Ion Detection in Solution and Solid State. *Adv. Funct. Mater.* **2016**, *26*, 514–523

(167) Moser, M.; Thorley, K. J.; Moruzzi, F.; Ponder, J. F.; Maria, I. P.; Giovannitti, A.; Inal, S.; McCulloch, I. Highly Selective Chromoionophores for Ratiometric Na^+ Sensing Based on an Oligoethyleneglycol Bridged Bithiophene Detection Unit. *J. Mater. Chem. C* **2019**, *7*, 5359–5365

(168) Parr, Z. S.; Nielsen, C. B. Conjugated Molecules for Colourimetric and Fluorimetric Sensing of Sodium and Potassium. *Mater. Chem. Front.* **2020**, *4*, 2370–2377

(169) Oike, T.; Kurata, T.; Takimiya, K.; Otsubo, T.; Aso, Y.; Zhang, H.; Araki, Y.; Ito, O. Polyether-Bridged Sexithiophene as a Complexation-Gated Molecular Wire for Intramolecular Photoinduced Electron Transfer. *J. Am. Chem. Soc.* **2005**, *127*, 15372–15373

(170) Demeter, D.; Blanchard, P.; Allain, M.; Grosu, I.; Roncali, J. Synthesis and Metal Cation Complexing Properties of Crown-Annelated Terthiophenes Containing 3,4-Ethylenedioxythiophene. *J. Org. Chem.* **2007**, *72*, 5285–5290

(171) Licchelli, M.; Biroli, A. O.; Poggi, A. A Prototype for the Chemosensing of Ba^{2+} Based on Self-Assembling Fluorescence Enhancement. *Org. Lett.* **2006**, *8*, 915–918

(172) Weißenstein, A.; Würthner, F. Metal Ion Templated Self-Assembly of Crown Ether Functionalized Perylene Bisimide Dyes. *Chem. Commun.* **2015**, *51*, 3415–3418

(173) Lu, X.; Zhu, W.; Xie, Y.; Li, X.; Gao, Y.; Li, F.; Tian, H. Near-IR Core-Substituted Naphthalenediimide Fluorescent Chemosensors for Zinc Ions: Ligand Effects on PET and ICT Channels. *Chem. - A Eur. J.* **2010**, *16*, 8355–8364

(174) Selector, S.; Fedorova, O.; Lukovskaya, E.; Anisimov, A.; Fedorov, Y.; Tarasova, N.; Raitman, O.; Fages, F.; Arslanov, V. Supramolecular Control of Photochemical and

Electrochemical Properties of Two Oligothiophene Derivatives at the Air/Water Interface. *J. Phys. Chem. B* **2012**, *116*, 1482–1490

(175) Molad, A.; Goldberg, I.; Vigalok, A. Tubular Conjugated Polymer for Chemosensory Applications. *J. Am. Chem. Soc.* **2012**, *134*, 7290–7292

(176) Zhu, S. S.; Swager, T. M. Conducting Polymetallorotaxanes: Metal Ion Mediated Enhancements in Conductivity and Charge Localization. *J. Am. Chem. Soc.* **1997**, *119*, 12568–12577

(177) Zhao, F.; Wang, Z.; Zhang, J.; Zhu, X.; Zhang, Y.; Fang, J.; Deng, D.; Wei, Z.; Li, Y.; Jiang, L.; Wang, C. Self-Doped and Crown-Ether Functionalized Fullerene as Cathode Buffer Layer for Highly-Efficient Inverted Polymer Solar Cells. *Adv. Energy Mater.* **2016**, *6*, 1502120

(178) Li, N.; Chen, F.; Shen, J.; Zhang, H.; Wang, T.; Ye, R.; Li, T.; Loh, T. P.; Yang, Y. Y.; Zeng, H. Buckyball-Based Spherical Display of Crown Ethers for De Novo Custom Design of Ion Transport Selectivity. *J. Am. Chem. Soc.* **2020**, *142*, 21082–21090

(179) Huang, L.; Wang, Z.; Chen, J.; Wang, B.; Chen, Y.; Huang, W.; Chi, L.; Marks, T. J.; Facchetti, A. Porous Semiconducting Polymers Enable High-Performance Electrochemical Transistors. *Adv. Mater.* **2021**, *33*, 2007041

(180) Savva, A.; Hallani, R.; Cendra, C.; Surgailis, J.; Hidalgo, T. C.; Wustoni, S.; Sheelamanthula, R.; Chen, X.; Kirkus, M.; Giovannitti, A.; Salleo, A.; McCulloch, I.; Inal, S. Balancing Ionic and Electronic Conduction for High-Performance Organic Electrochemical Transistors. *Adv. Funct. Mater.* **2020**, *30*, 1907657

(181) Savva, A.; Cendra, C.; Giugni, A.; Torre, B.; Surgailis, J.; Ohayon, D.; Giovannitti, A.; McCulloch, I.; Di Fabrizio, E.; Salleo, A.; Rivnay, J.; Inal, S. Influence of Water on the Performance of Organic Electrochemical Transistors. *Chem. Mater.* **2019**, *31*, 927–937

(182) Stavrinidou, E.; Leleux, P.; Rajaona, H.; Khodagholy, D.; Rivnay, J.; Lindau, M.; Sanaur, S.; Malliaras, G. G. Direct Measurement of Ion Mobility in a Conducting Polymer. *Adv. Mater.*

2013, *25*, 4488–4493

(183) Inal, S.; Malliaras, G. G.; Rivnay, J. Optical Study of Electrochromic Moving Fronts for the Investigation of Ion Transport in Conducting Polymers. *J. Mater. Chem. C* **2016**, *4*, 3942–3947

(184) Rivnay, J.; Leleux, P.; Ferro, M.; Sessolo, M.; Williamson, A.; Koutsouras, D. A.; Khodagholy, D.; Ramuz, M.; Strakosas, X.; Owens, R. M.; Benar, C.; Badier, J.-M. J. M.; Bernard, C.; Malliaras, G. G. High-Performance Transistors for Bioelectronics through Tuning of Channel Thickness. *Sci. Adv.* **2015**, *1*, e1400251

(185) Inal, S.; Malliaras, G. G.; Rivnay, J. Benchmarking Organic Mixed Conductors for Transistors. *Nat. Commun.* **2017**, *8*, 1767

(186) Bischak, C. G.; Flagg, L. Q.; Yan, K.; Li, C. Z.; Ginger, D. S. Fullerene Active Layers for N-Type Organic Electrochemical Transistors. *ACS Appl. Mater. Interfaces* **2019**, *11*, 28138–28144

(187) Giovannitti, A.; Maria, I. P.; Hanifi, D.; Donahue, M. J.; Bryant, D.; Barth, K. J.; Makdah, B. E.; Savva, A.; Moia, D.; Zetek, M.; Barnes, P. R. F.; Reid, O. G.; Inal, S.; Rumbles, G.; Malliaras, G. G.; Nelson, J.; Rivnay, J.; McCulloch, I. The Role of the Side Chain on the Performance of N-Type Conjugated Polymers in Aqueous Electrolytes. *Chem. Mater.* **2018**, *30*, 2945–2953

(188) Flagg, L. Q.; Giridharagopal, R.; Guo, J.; Ginger, D. S. Anion-Dependent Doping and Charge Transport in Organic Electrochemical Transistors. *Chem. Mater.* **2018**, *30*, 5380–5389

(189) Flagg, L. Q.; Bischak, C. G.; Quezada, R. J.; Onorato, J. W.; Luscombe, C. K.; Ginger, D. S. P-Type Electrochemical Doping Can Occur by Cation Expulsion in a High-Performing Polymer for Organic Electrochemical Transistors. *ACS Mater. Lett.* **2020**, *2*, 254–260

(190) Matta, M.; Wu, R.; Paulsen, B. D.; Petty II, A. J.; Sheelamanthula, R.; McCulloch, I.; Schatz, G. C.; Rivnay, J. Ion Coordination and Chelation in a Glycolated Polymer Semiconductor:

Molecular Dynamics and X-Ray Fluorescence Study. *Chem. Mater.* **2020**, *32*, 7301–7308

(191) Paulsen, B. D.; Wu, R.; Takacs, C. J.; Steinrück, H. G.; Strzalka, J.; Zhang, Q.; Toney, M. F.; Rivnay, J. Time-Resolved Structural Kinetics of an Organic Mixed Ionic–Electronic Conductor. *Adv. Mater.* **2020**, *32*, 2003404

(192) Sun, H.; Vagin, M.; Wang, S.; Crispin, X.; Forchheimer, R.; Berggren, M.; Fabiano, S. Complementary Logic Circuits Based on High-Performance n-Type Organic Electrochemical Transistors. *Adv. Mater.* **2018**, *30*, 1704916

(193) Surgailis, J.; Savva, A.; Druet, V.; Paulsen, B. D.; Wu, R.; Hamidi-Sakr, A.; Ohayon, D.; Nikiforidis, G.; Chen, X.; McCulloch, I.; Rivnay, J.; Inal, S. Mixed Conduction in an N-Type Organic Semiconductor in the Absence of Hydrophilic Side-Chains. *Adv. Funct. Mater.* **2021**, *31*, 2010165

(194) Ruzié, C.; Karpinska, J.; Laurent, A.; Sanguinet, L.; Hunter, S.; Anthopoulos, T. D.; Lemaur, V.; Cornil, J.; Kennedy, A. R.; Fenwick, O.; Samorì, P.; Schweicher, G.; Chattopadhyay, B.; Geerts, Y. H. Design, Synthesis, Chemical Stability, Packing, Cyclic Voltammetry, Ionisation Potential, and Charge Transport of [1]Benzothieno[3,2-*b*][1]Benzothiophene Derivatives. *J. Mater. Chem. C* **2016**, *4*, 4863–4879

(195) Hallani, R. K.; Thorley, K. J.; Mei, Y.; Parkin, S. R.; Jurchescu, O. D.; Anthony, J. E. Structural and Electronic Properties of Crystalline, Isomerically Pure Anthradithiophene Derivatives. *Adv. Funct. Mater.* **2016**, *26*, 2341–2348

(196) Oh, J. Y.; Rondeau-Gagné, S.; Chiu, Y.-C.; Chortos, A.; Lissel, F.; Wang, G.-J. N.; Schroeder, B. C.; Kurosawa, T.; Lopez, J.; Katsumata, T.; Xu, J.; Zhu, C.; Gu, X.; Bae, W.-G.; Kim, Y.; Jin, L.; Chung, J. W.; Tok, J. B.-H.; Bao, Z. Intrinsically Stretchable and Healable Semiconducting Polymer for Organic Transistors. *Nature* **2016**, *539*, 411–415

(197) Wang, Y.; Zeglio, E.; Liao, H.; Xu, J.; Liu, F.; Li, Z.; Maria, I. P.; Mawad, D.; Herland, A.; McCulloch, I.; Yue, W. Hybrid Alkyl-Ethylene Glycol Side Chains Enhance Substrate

Adhesion and Operational Stability in Accumulation Mode Organic Electrochemical Transistors. *Chem. Mater.* **2019**, *31*, 9797–9806

(198) Zeglio, E.; Vagin, M.; Musumeci, C.; Ajjan, F. N.; Gabrielsson, R.; Trinh, X. T.; Son, N. T.; Maziz, A.; Solin, N.; Inganäs, O. Conjugated Polyelectrolyte Blends for Electrochromic and Electrochemical Transistor Devices. *Chem. Mater.* **2015**, *27*, 6385–6393

(199) Zeglio, E.; Eriksson, J.; Gabrielsson, R.; Solin, N.; Inganäs, O. Highly Stable Conjugated Polyelectrolytes for Water-Based Hybrid Mode Electrochemical Transistors. *Adv. Mater.* **2017**, *29*, 1605787

(200) Pulido, A.; Chen, L.; Kaczorowski, T.; Holden, D.; Little, M. A.; Chong, S. Y.; Slater, B. J.; McMahon, D. P.; Bonillo, B.; Stackhouse, C. J.; Stephenson, A.; Kane, C. M.; Clowes, R.; Hasell, T.; Cooper, A. I.; Day, G. M. Functional Materials Discovery Using Energy-Structure-Function Maps. *Nature* **2017**, *543*, 657–664

(201) Armitage, J.; Spalek, L. J.; Nguyen, M.; Nikolka, M.; Jacobs, I. E.; Marañón, L.; Nasrallah, I.; Schweicher, G.; Dimov, I.; Simatos, D.; McCulloch, I.; Nielsen, C. B.; Conduit, G.; Sirringhaus, H. Fragment Graphical Variational Autoencoding for Screening Molecules with Small Data. *arXiv*. **2019**, arXiv:1910.13325v2

(202) McCulloch, I.; Heeney, M.; Bailey, C.; Genevicius, K.; MacDonald, I.; Shkunov, M.; Sparrowe, D.; Tierney, S.; Wagner, R.; Zhang, W.; Chabinyc, M. L.; Kline, R. J.; McGehee, M. D.; Toney, M. F. Liquid-Crystalline Semiconducting Polymers with High Charge-Carrier Mobility. *Nat. Mater.* **2006**, *5*, 328–333

(203) Guardado, J. O.; Salleo, A. Structural Effects of Gating Poly(3-Hexylthiophene) through an Ionic Liquid. *Adv. Funct. Mater.* **2017**, *27*, 1701791

(204) Duong, D. T.; Tuchman, Y.; Chakthranont, P.; Cavassin, P.; Colucci, R.; Jaramillo, T. F.; Salleo, A.; Faria, G. C. A Universal Platform for Fabricating Organic Electrochemical Devices. *Adv. Electron. Mater.* **2018**, *4*, 1800090

(205) Sessolo, M.; Rivnay, J.; Bandiello, E.; Malliaras, G. G.; Bolink, H. J. Ion-Selective Organic Electrochemical Transistors. *Adv. Mater.* **2014**, *26*, 4803–4807

(206) Parlak, O.; Keene, S. T.; Marais, A.; Curto, V. F.; Salleo, A. Molecularly Selective Nanoporous Membrane-Based Wearable Organic Electrochemical Device for Noninvasive Cortisol Sensing. *Sci. Adv.* **2018**, *4*, eaar2904

(207) Wustoni, S.; Combe, C.; Ohayon, D.; Akhtar, M. H.; McCulloch, I.; Inal, S. Membrane-Free Detection of Metal Cations with an Organic Electrochemical Transistor. *Adv. Funct. Mater.* **2019**, *29*, 1904403